Chapter 6 High Resolution TEM

- K. Ishizuka (1980) ***"Contrast Transfer of Crystal Images in TEM"***, Ultramicroscopy **5**,pages 55-65.
- L. Reimer (1993) ***"Transmission Electron Microscopy"***, Springer Verlag, Berlin.
- J.C.H. Spence (1988), ***"Experimental High Resolution Electron Microscopy"***, Oxford University Press, New York.

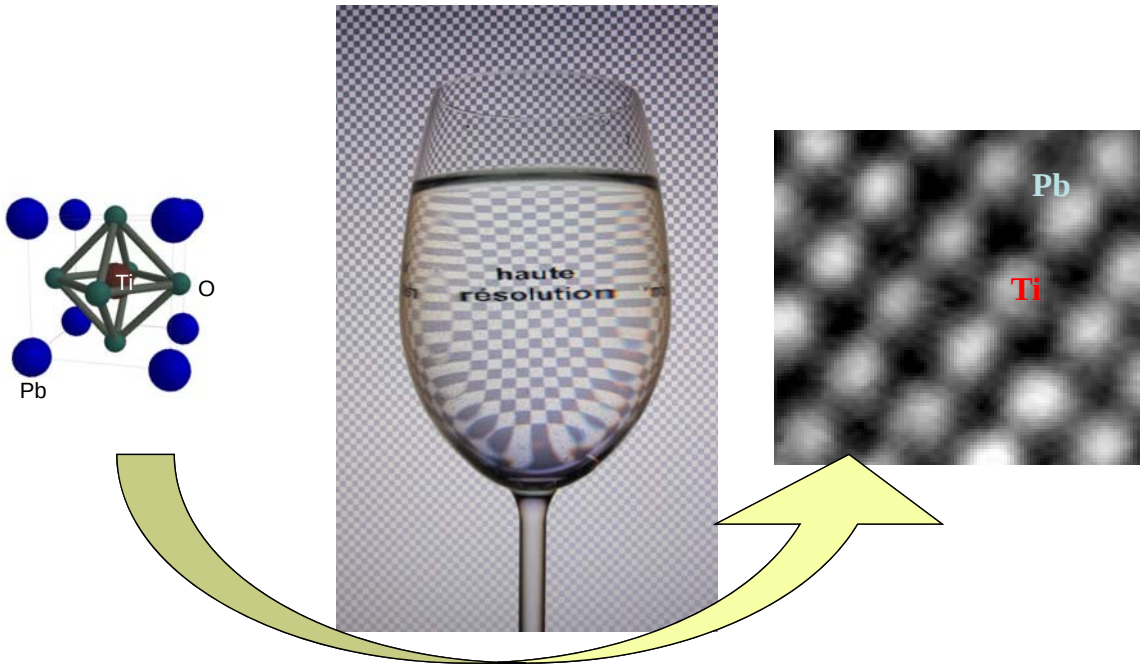

Summary

Contrast in TEM images results from the scattering of electrons in thin samples and changes in the phase of the electron waves. When 2 or more electrons beams scattered from the sample interfere and are transferred at high magnification to detector plane, there can form an interference pattern that we commonly refer as a high resolution TEM image. The phase shift of the electron waves can be used to map the atomic structure of the sample which appear as fringes (2 scattered beams) or white and dark spot patterns (>2 beams). The contrast mechanisms are difficult to interpret being very sensitive to many factors such as thickness, orientation and scattering of the sample, objective lens focus and aberrations, electron beam coherence and convergence angle on the sample. As such, we need simulations to interpret them properly.

HREM TEM simulations are needed to interpret the contrast mechanisms and complicated Interference Patterns of HRTEM IMAGES. Through careful experimentation, image acquisition and simulation of HRTEM images, we can reconstruct the projected potential of the specimen and determine its atomic structure. The common method for simulating HRTEM images is the multi-slice calculation in which the sample volume is sliced into sections and the associated phase shift due to scattering from the sample's crystal structure is sequentially calculated for each slice. The calculation can take into account the microscope performance and experimental conditions, such as aberrations, objective lens defocus and sample thickness. Because the HRTEM phase contrast is very sensitive to defocus and sample thickness and it is difficult to known these parameters experimentally with the required precision, we can simulate montages of HRTEM images that illustrate the variance in the pattern with defocus and thickness which can be compared to the experimental data.

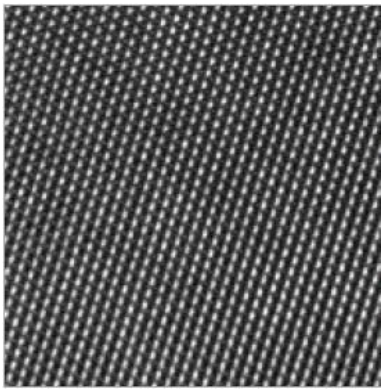

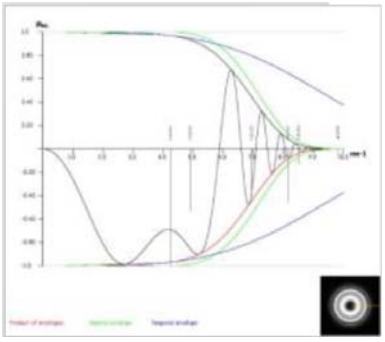

CIME Talos, modern TEM

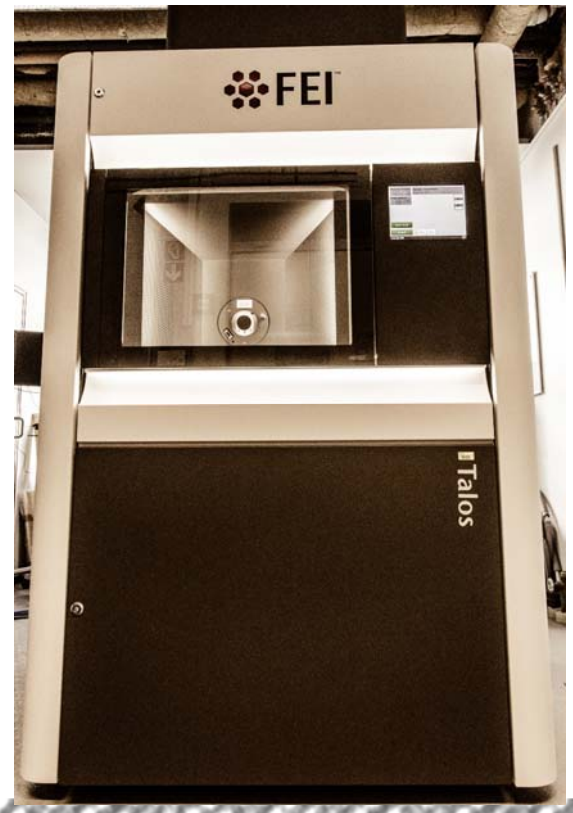

Talos F200S at CIME-EPFL	
Electron Gun	S-FEG
Lens System	Constant Power
EDS System	2-SDD
Specimen loading	Remote with touch screen
STEM HAADF resolution	0.16 nm
TEM Information limit	0.12 nm
TEM point to point resolution	0.24 nm
Camera	CMOS (CETA)

Examples form Talos

- Nanowire with defects

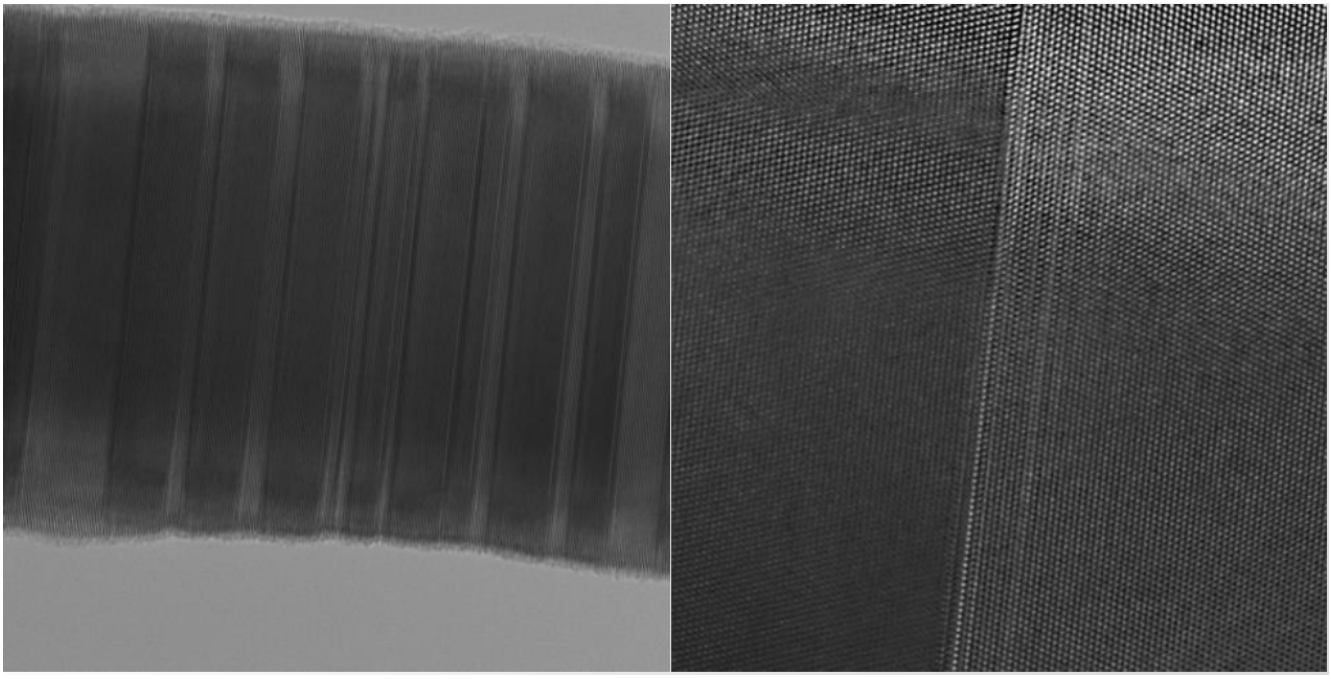

Nanowire oxide

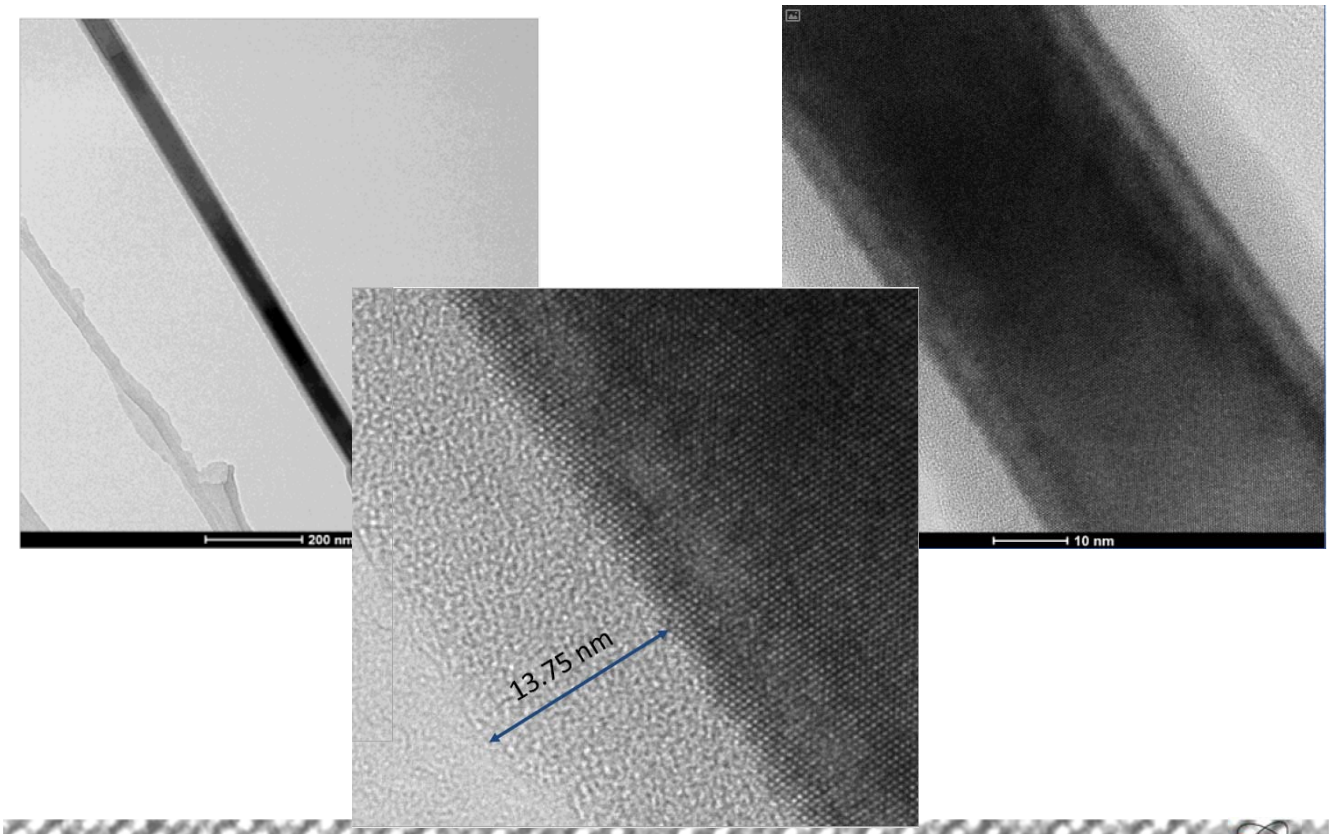

Analysis of thin films

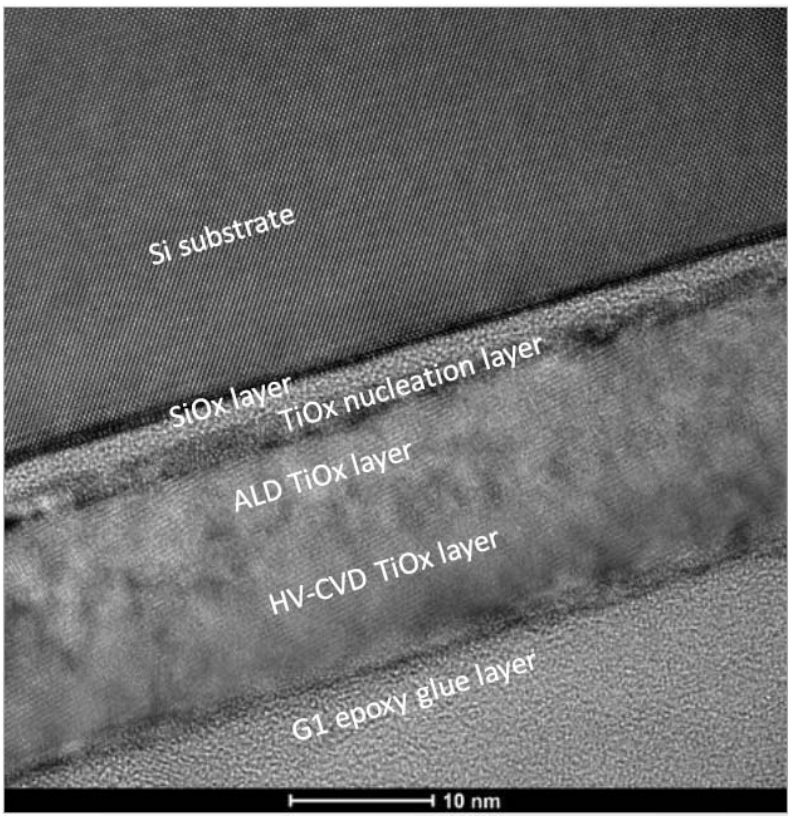

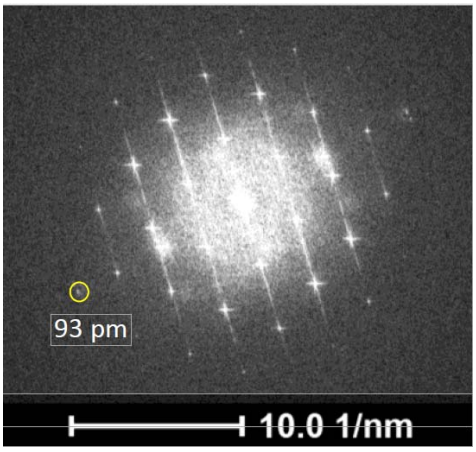

Bright Field Imaging

Diffraction Contrast, Au (nano-) particles on C film

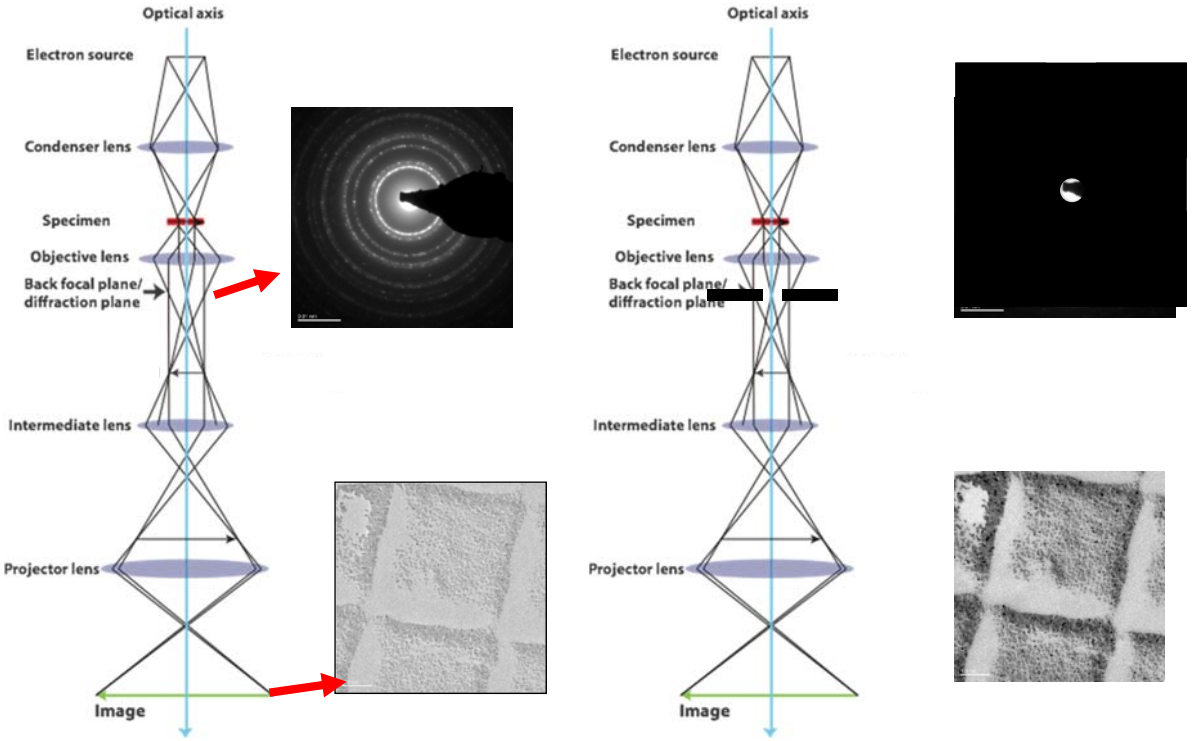

High resolution….?!

electron at 300keV:

- v = 2.33 10^{-8} m/s (0.78 c)
- λ = 0.00197nm
- θ_{diff} = 10^{-3} rad

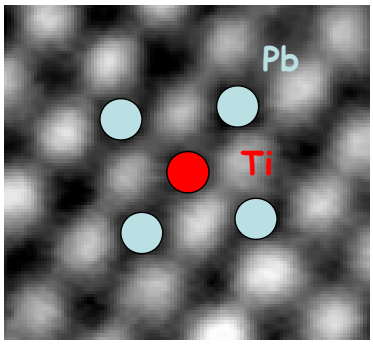

Atomic resolution…?

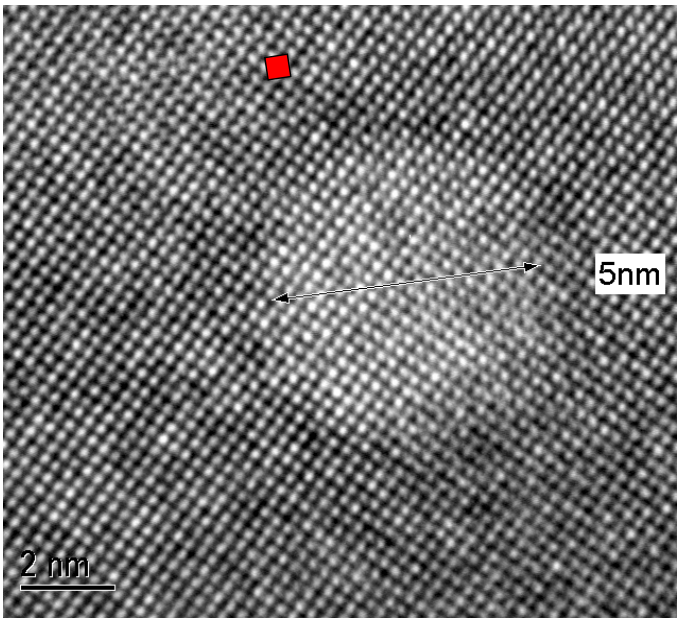

Precipitate in a ceramic: $PbTiO_3$

Scherzer-defocus: “black-atom” contrast

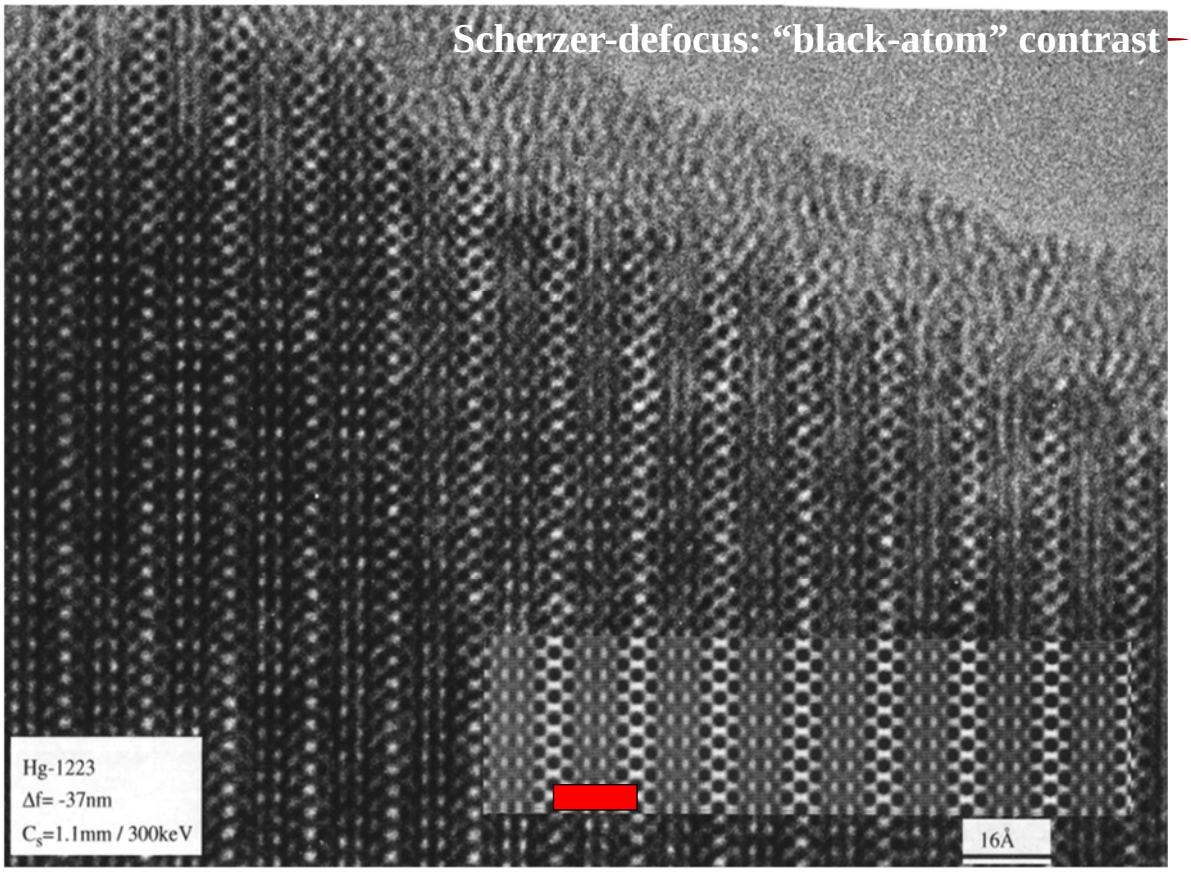

“White-atom” contrast

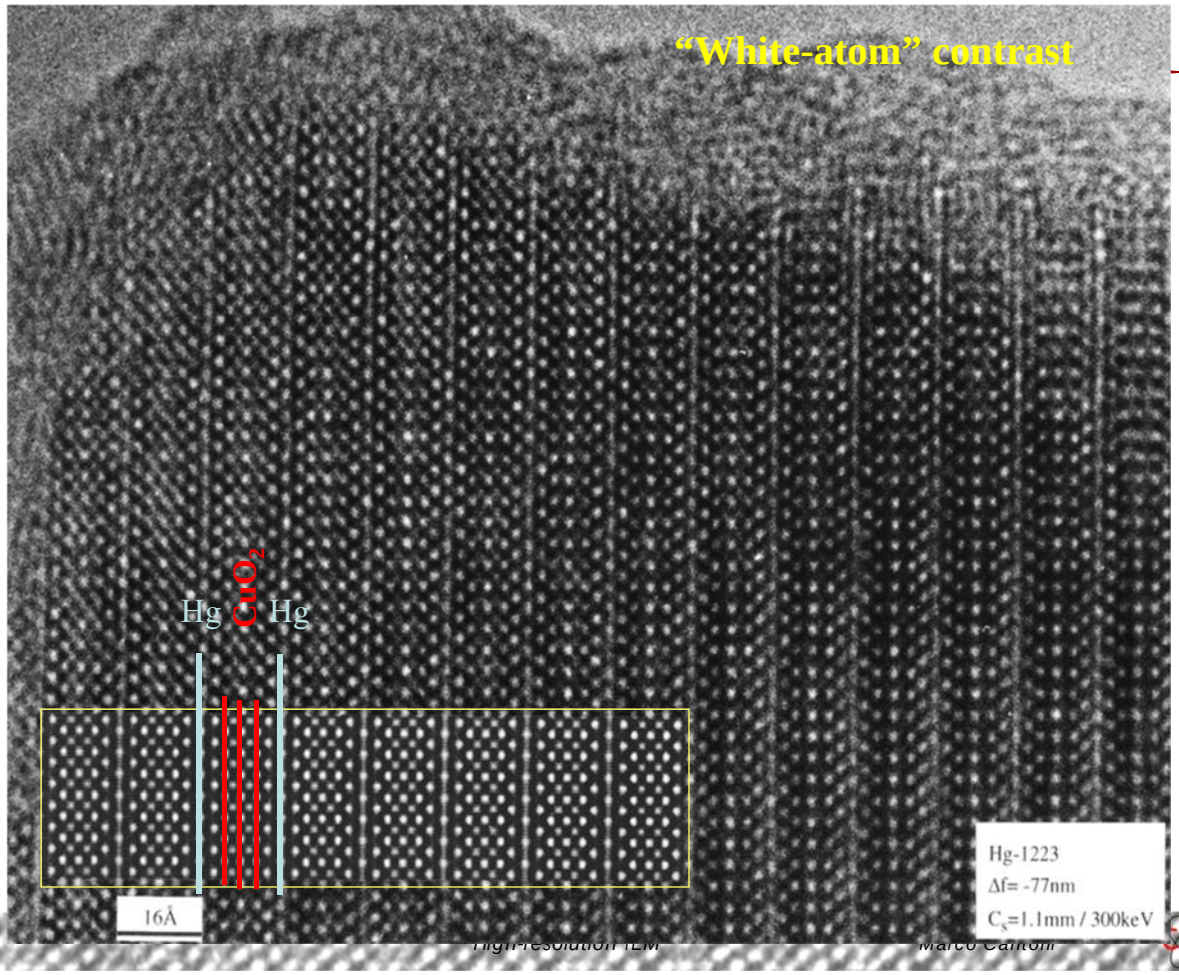

High-resolution

- The image should ressemble the atomic structure !
- Atomes…?
  Thin samples: atom columns: orientation of the sample (incident beam // atom columns)
- The observed contrast varies with thickness and defocalisation…!
- Need to compare with simulations !

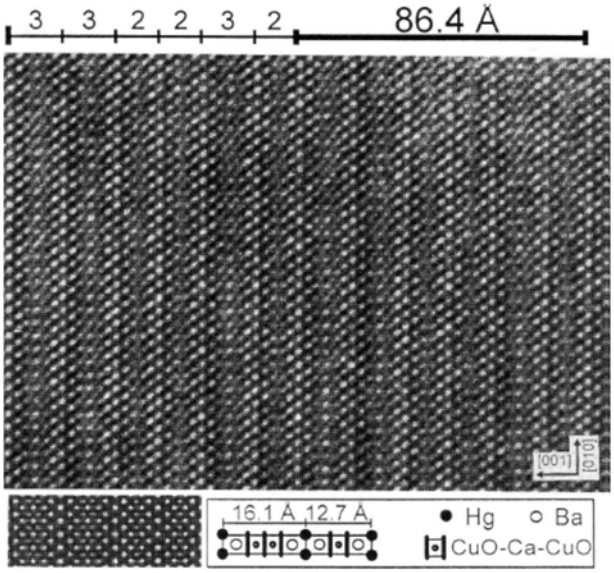

the TEM in "high-resolution" mode

A high-resolution image is an interference image of the transmitted and the diffracted beams!

Diffracted electrons: coherent elastic scattering (the electrons have seen the crystal lattice)

The quality of the image depends on the optical system that makes the beams interfere

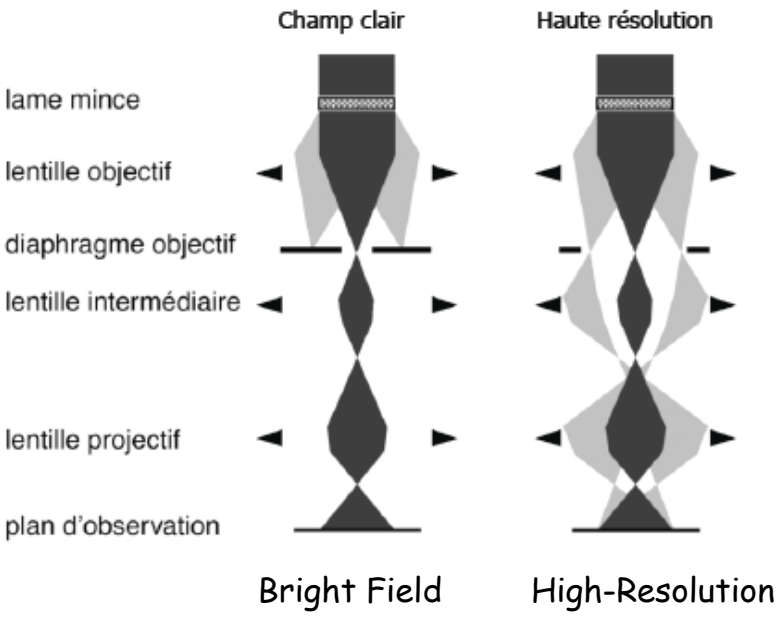

The objective lens

- Field with rotational symmetry
- Lorenz Force : **F** = -e **v** ^ **B**
  e on optical axis: **F** = 0
  e not on optical axis : deviated
  optical axis: symmetry axis

- **Scherzer 1936:**
- Magnetic lens with rotational symmetry:

Aberration coefficients:

C_s: spherical

C_c: chromatical

- Always positive !!

$$C_s = \frac{1}{16}\int_{z_0}^{z_1}\{b^4h^4 + 2(hb' + h'b)^2h^2 + 2b^2h^2h'^2\}dz$$

$$C_c = \frac{1}{4}\int_{z_0}^{z_1} b^2h^2dz$$

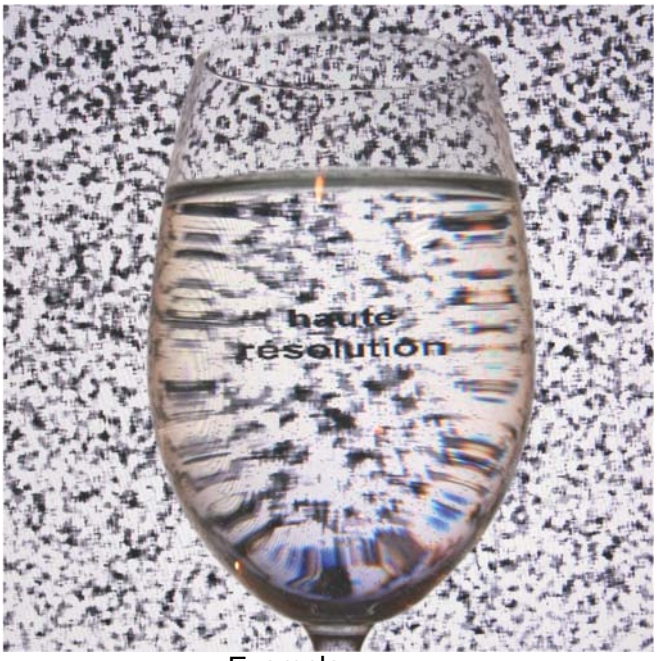

Resolution limit: $D_{res} = 0.66\lambda^{3/4}C_s^{1/4}$

Example:

λ= 0.00197nm, C_s = 1 mm

D_{res} = 1.8 10^{-10} = 1.8Å

Image formation

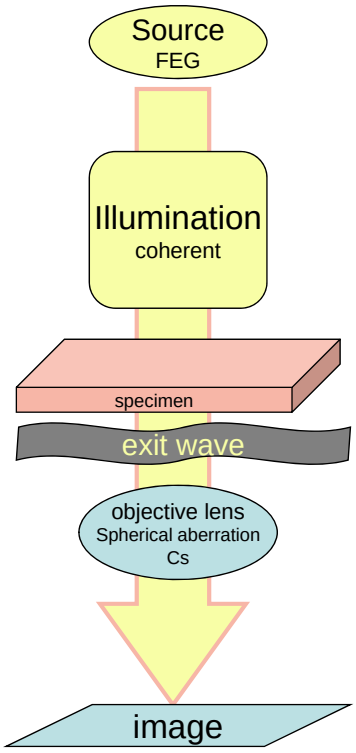

- **Source:** *coherent and monochromatic*
- **Illumination:** *parallel*
- **Sample:** thin, *nicely prepared (no amorphization), orientation (zone axis)*
- **objective lens:** *aberrations, focus, stability !*
- **projection** lens system *(magnification)*

Image formation

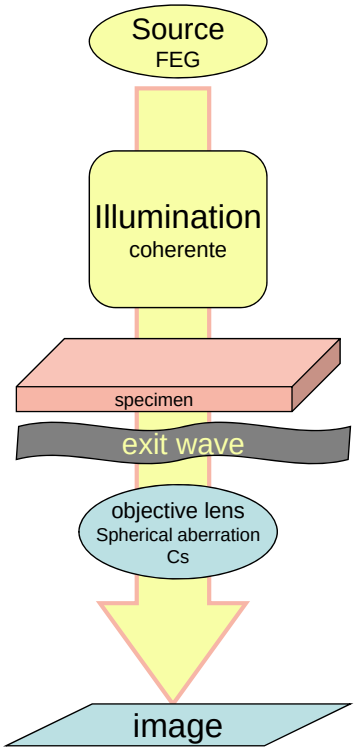

- **Illumination:** *parallel beam*

$$\Psi(\vec{\mathbf{r}}) = \Psi_0 \exp^{2\pi i \vec{\mathbf{k}}\cdot\vec{\mathbf{r}}}$$

- **Sample:**

weak phase object:
weak phase object aproximation (WPOA)

- **Objective lens:**

Abbé's principle
transfert function
coherent transfer function (CTF)

$$\Psi_i(\vec{\mathbf{x}}) = \Psi_o(\vec{\mathbf{x}}) \otimes T(\vec{\mathbf{x}})$$

- **Image contrast** (intensity)

$$\mathrm{I}_i(\vec{\mathbf{x}}) = \Psi_i(\vec{\mathbf{x}})\Psi_i^*(\vec{\mathbf{x}})$$

sample = phase objet

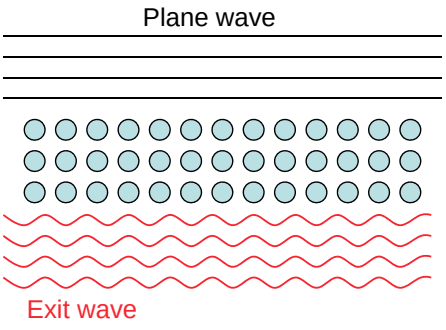

Wave vector in vacuum:

$$k = \sqrt{2me(E)/h^2}$$

Wave vector in a potential:

$$k = \sqrt{2me(E + V(\vec{r}))/h^2}$$

Phase shift $\Delta\alpha$ due to the cristal potential V_p:

$$\Delta\alpha = \frac{\sigma}{2\pi} V_p(\vec{x}, z)$$

$$\sigma = \pi/\lambda E$$

Exit wave function:

$$\Psi_o(\vec{\mathbf{x}}) = exp\left[-i\sigma V_p(\vec{\mathbf{x}}; z)\right]$$

WPOA

- Weak phase object approximation:

$$\Psi_o(\vec{\mathbf{x}}) = exp\left[-i\sigma V_p(\vec{\mathbf{x}};z)\right] \cong 1 - i\sigma V_p(\vec{\mathbf{x}};z)$$

No absorbtion,effect of the object on the outgoing wave: only phase shift

The exit wave function contains the information about the structure of the sample

Multi-slice calculation:

Calculation of the exit wave function for complex structures:

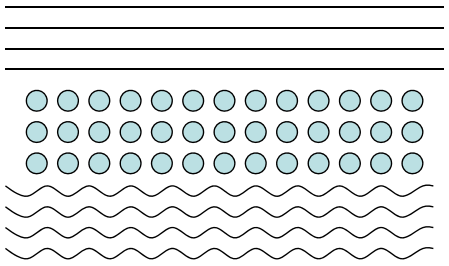

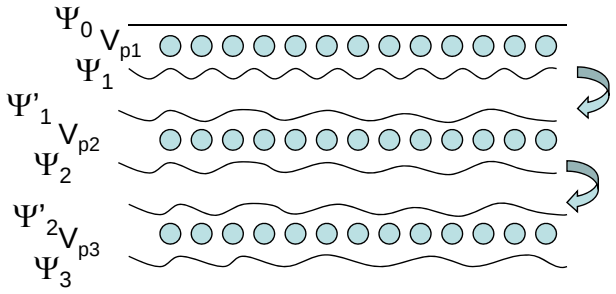

The sample is cut into thin slices

Transfer Function

- The optical system (lenses) can be described by a convolution with a transfer function T(x):
  Point spread function (PSF): describes how a point on the object side is transformed into the image.

$$\Psi_i(\underline{x}) = \int_{-\infty}^{\infty} \Psi_o(\underline{u})T(\underline{x}-\underline{u})d\underline{u} = \Psi_o(\underline{x}) \otimes T(\underline{x})$$

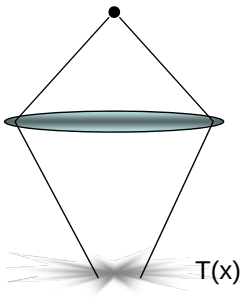

- ***Transfer Function***:
  desscribe how an "objet" wave-function is transformed into an "image" wave-function

$$\Psi_i(\underline{h}) = \Psi_o(\underline{h})T(\underline{h})$$

- **The image INTENSITY** observed on a screen (or a camera / negative plate etc.)

$$I_i(\underline{x}) = \Psi_i(\underline{x})\Psi_i^*(\underline{x}) \qquad I_i(\underline{h}) = \Psi_i(\underline{h}) \otimes \Psi_i^*(-\underline{h}) = \int \Psi_i(\underline{h}')\Psi_i^*(\underline{h}-\underline{h}')d\underline{h}'$$

$$I_i(\underline{h}) = [\Psi_o(\underline{h})T(\underline{h})] \otimes [\Psi_o^*(-\underline{h})T^*(-\underline{h})]$$

Abbé's principle

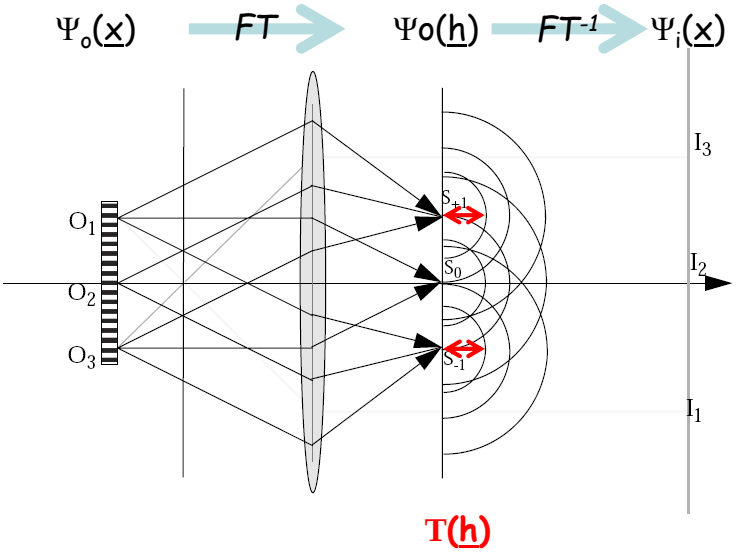

Principe de la formation de l'image proposé pour la première fois par Abbé. L'onde incidente monochromatique est diffractée par l'objet. Le diagramme de Fraunhofer de la fonction d'onde de l'objet est formé dans le plan focal image de la lentille, plan dans lequel la fonction de transfert de la lentille est T(**h**). L'image I_i de l'objet O_i est le résultat de l'interférence des ondelettes secondaires émises par des sources ponctuelles S_i placées dans le plan focal image de la lentille.

Transfer Function

$$T(\vec{\mathbf{h}}) = a(\vec{\mathbf{h}}) \exp\left[2\pi i \chi(\vec{\mathbf{h}})\right] E_s(\vec{\mathbf{h}}) E_t(\vec{\mathbf{h}})$$

- Phase factors:
  - Spherical Aberration
  - Defocus
- Amplitude factors:
  - (objective) apertures
  - spatial coherence enveloppe (non-parallel, convergent beam)
  - Temporal coherence envelope (non monochromatic beam, instabilities of the gun and lenses)

Transfer Function

$$T(\vec{\mathbf{h}}) = \exp\left[2\pi i \chi(\vec{\mathbf{h}})\right]$$

$$\chi(\vec{\mathbf{h}}) = 0.25 C_s \lambda^3 h^4 + 0.5 \Delta z \lambda h^2$$

Spherical aberration — defocus

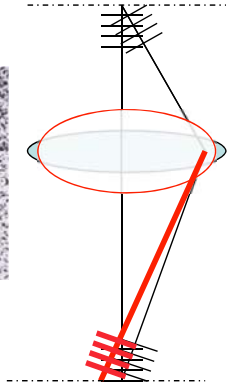

Object plane

image plane

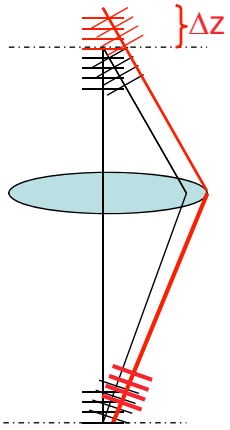

Image formation

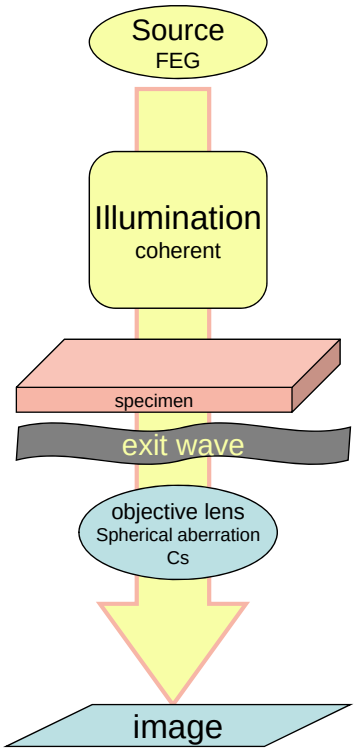

- Illumination

$$\Psi(\vec{\mathbf{r}}) = \Psi_0 \exp^{2\pi i \vec{\mathbf{k}}\cdot\vec{\mathbf{r}}}$$

- Sample

$$\Psi_o(\vec{\mathbf{x}}) = exp\left[-i\sigma V_p(\vec{\mathbf{x}};z)\right] \cong 1 - i\sigma V_p(\vec{\mathbf{x}};z)$$

- objective lens

$$T(\vec{\mathbf{h}}) = \exp\left[2\pi i \chi(\vec{\mathbf{h}})\right] \quad avec \quad \chi(\vec{\mathbf{h}}) = 0.25 C_s \lambda^3 h^4 + 0.5 \Delta z \lambda h^2$$

$$\Psi_i(\vec{\mathbf{x}}) = \Psi_o(\vec{\mathbf{x}}) \otimes T(\vec{\mathbf{x}})$$

- Image, contrast

$$\mathrm{I}_i(\vec{\mathbf{x}}) = \Psi_i(\vec{\mathbf{x}}) \Psi_i^*(\vec{\mathbf{x}})$$

The « magic » of image contrast

Weak phase object

$$\Psi_o(\underline{x}) = exp[-i\sigma V_p(\underline{x};z)] \cong 1 - i\sigma V_p(\underline{x};z)$$

$$\Psi_o(\underline{h}) = \delta(\underline{h}) - i\sigma V_p(\underline{h})$$

$$\Psi_i(\underline{h}) = \Psi_o(\underline{h})T(\underline{h}) = \Psi_o(\underline{h})exp[2\pi i\chi(\underline{h})]$$

$$\Psi_i(\underline{h}) = [\delta(\underline{h}) - i\sigma V_p(\underline{h})][\cos 2\pi\chi(\underline{h}) + i\sin 2\pi\chi(\underline{h})]$$

Fourier Space

Selecting $\sin[2\pi\chi(\underline{\mathbf{h}})] = -1$, $\cos[2\pi\chi(\underline{\mathbf{h}})] = 0$ ***for the strongest reflections*** $\underline{h}$

Image wave function

$$\Psi_i(\underline{h}) = \delta(\underline{h}) - \sigma V_p(\underline{h})$$

The image intensity $\Psi_i(\underline{x})\,\Psi_i^*(\underline{x}))$ ***is given by :***

Intensity of a weak phase objet in "direct" contrast

$$I(\underline{x}) = (1 - \sigma V_p(\underline{x}))(1 + \sigma V_p(\underline{x})) = 1 - 2\sigma V_p(\underline{x}) + O(\sigma^2 V_p^2(\underline{x}))$$

but....

Selecting $\sin[2\pi\chi(\underline{\mathbf{h}})] = 0$, $\cos[2\pi\chi(\underline{\mathbf{h}})] = 1$. ***for the strongest reflections*** $\underline{h}$

Image wave function

$$\Psi_i(\underline{h}) = [\delta(\underline{h}) - i\sigma V_p(\underline{h})]$$

Intensity of a weak phase objet in "reversed" contrast

$$I(\underline{x}) = (1 - i\sigma V_p(\underline{x}))(1 + i\sigma V_p(\underline{x})) = 1 + \sigma^2 V_p^2(\underline{x})$$

Intensity is proportional to the square of the projected potential V_p ***: Image interpretation in terms of atom columns becomes complicated….***

For a direct and simple interpretation of the image contrast:
the imaginary part (sin) of the transfer function exp[2pic(h)] should be ~1

The only free parameter in the microscope is: the defocus Dz

CTF

- CTF: contrast transfer function (« useful part » = V_p)

$$T(\vec{\mathbf{h}}) = \exp\left[2\pi i \chi(\vec{\mathbf{h}})\right]$$
$$\chi(\vec{\mathbf{h}}) = 0.25 C_s \lambda^3 h^4 + 0.5 \Delta z \lambda h^2$$

$$CTF(h) = -\sin\left[\frac{\pi}{2} C_s \lambda^3 h^4 + \pi \Delta z \lambda h^2\right]$$

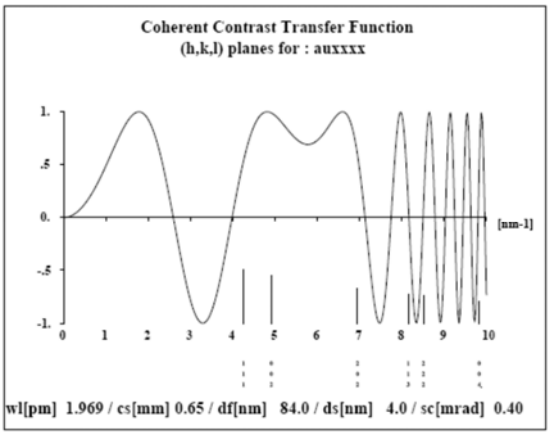

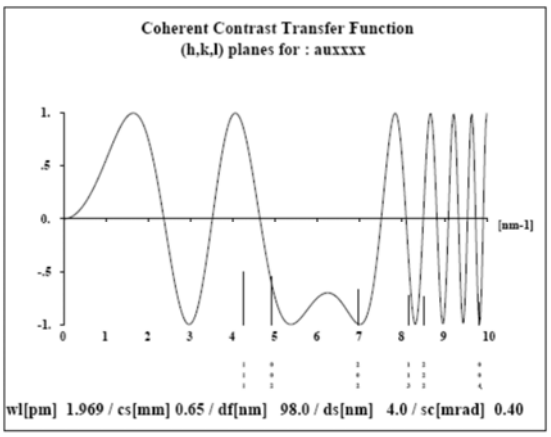

« Scherzer Defocus »

With $\Delta z_{scherzer}$

$$\Delta z = -\sqrt{4/3\, C_s \lambda}$$

The CTF has a wide pass band

$$D_{scherzer} = 0.66 \lambda^{3/4} C_s^{1/4}$$

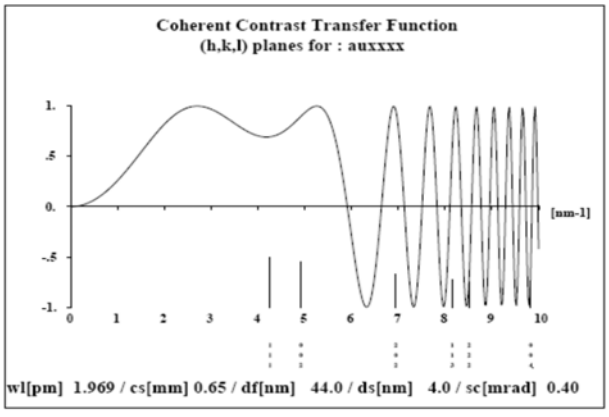

The first zero crossing of the CTF defines the « point-to-point » resolution of an electron microscope
The atom columns appear as dark areas on a bright background

$$I(\underline{x}) = (1 - \sigma V_p(\underline{x}))(1 + \sigma V_p(\underline{x})) = 1 - 2\sigma V_p(\underline{x}) + O(\sigma^2 V_p^2(\underline{x}))$$

Spatial and temporal coherence

$$T(\vec{\mathbf{h}}) = a(\vec{\mathbf{h}})\exp\left[2\pi i\chi(\vec{\mathbf{h}})\right]E_s(\vec{\mathbf{h}})E_t(\vec{\mathbf{h}})$$

CM300UT FEG
Field emission
C_s: 0.7mm
Dz= 44nm

Resolution (point to point):
1.7Å
Information limit : ~1.2Å

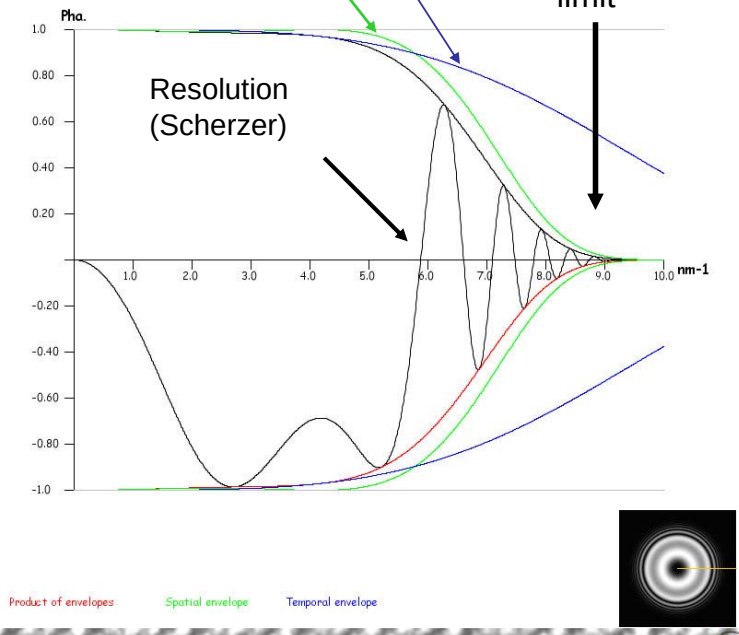

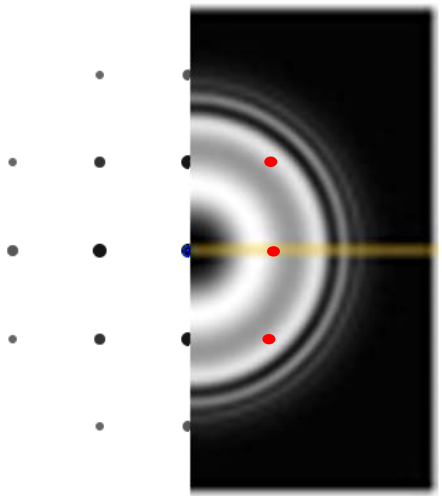

A good (old) microscope

CM300UT FEG
Field emission
C_s: 0.7mm
Δz= 44nm

Resolution (point to point): 1.7Å
Information limit: ~1.2Å

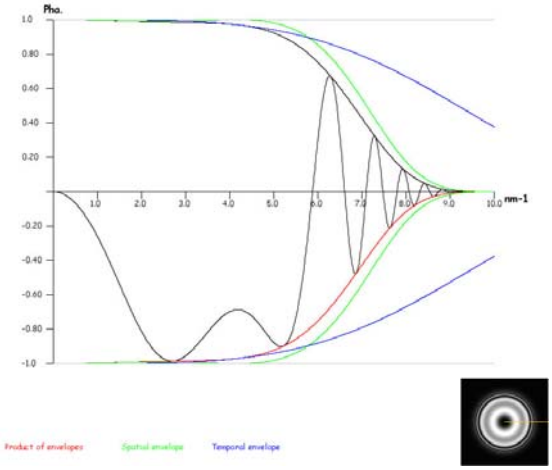

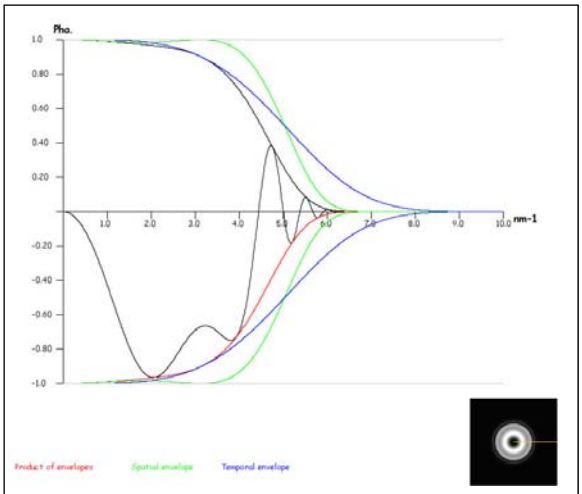

CM30ST LaB6
Thermal emitter
C_s: 2mm
Δz= 76nm

Resolution (point to point): 2.1Å
information limit: ~1.9Å

Pass bands

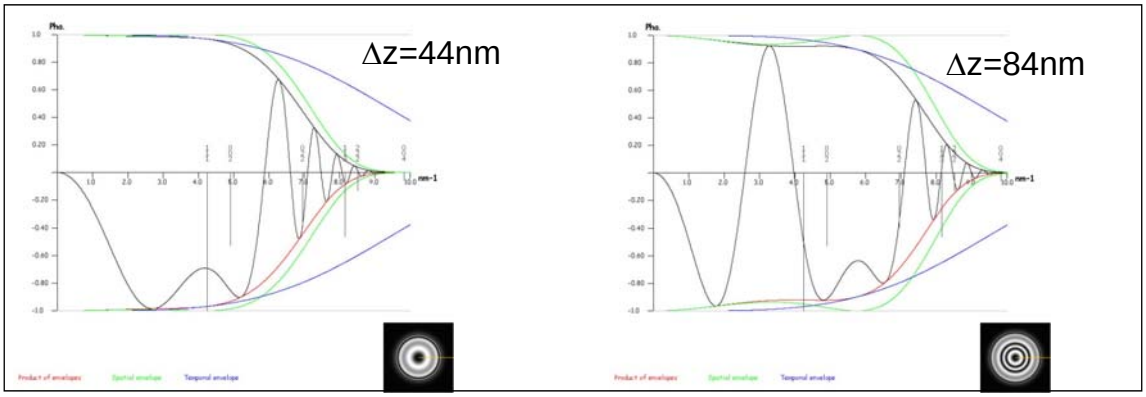

direct

Réflexions hkl pour Au

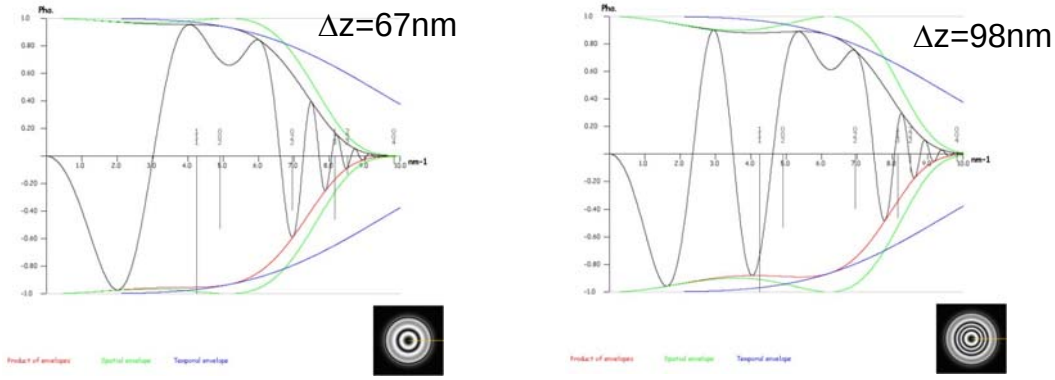

Defocus

defocus

Wave funct.

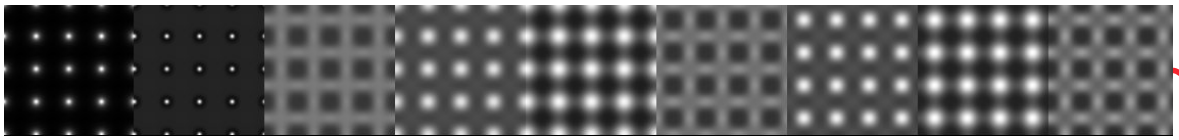

proj. pot. scherzer 1. p.b. 2. p.b.

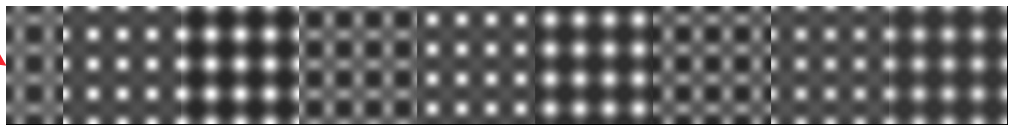

3. p.b.

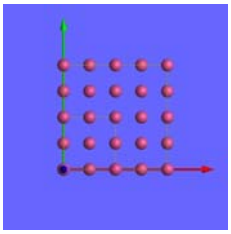

Au [100], thickness 20nm

HRTEM image formation

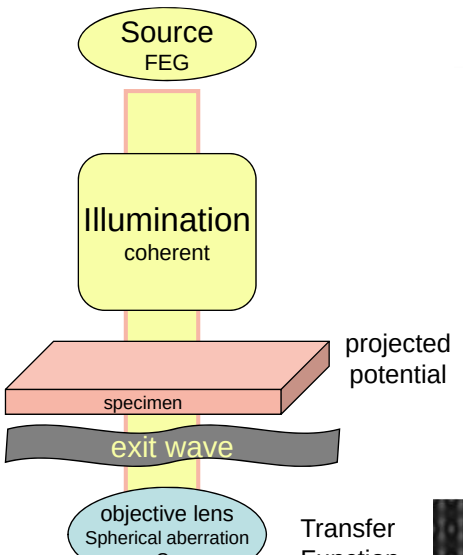

projected potential

Transfer Function

image of "projected potential"

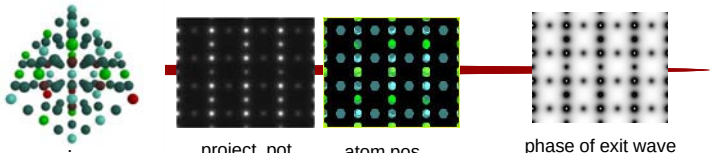

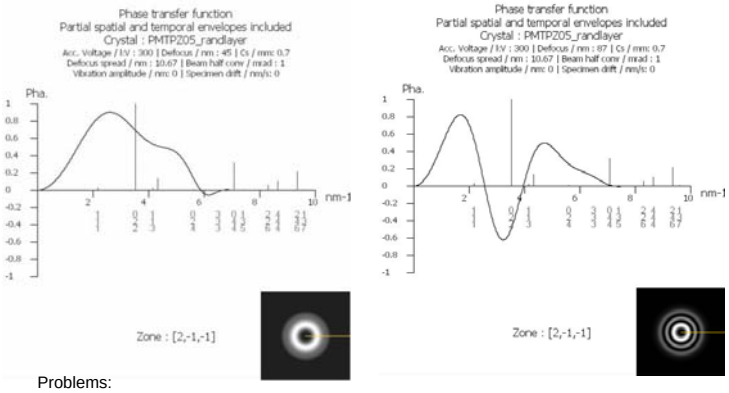

Problems:
defocusing for contrast: delocalization of information, information limit not used

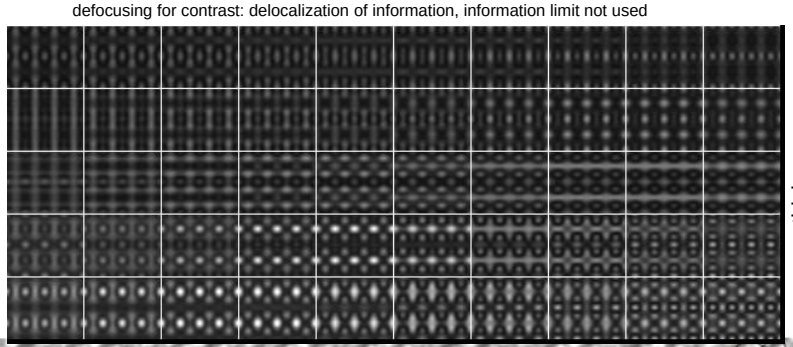

thickness

defocus

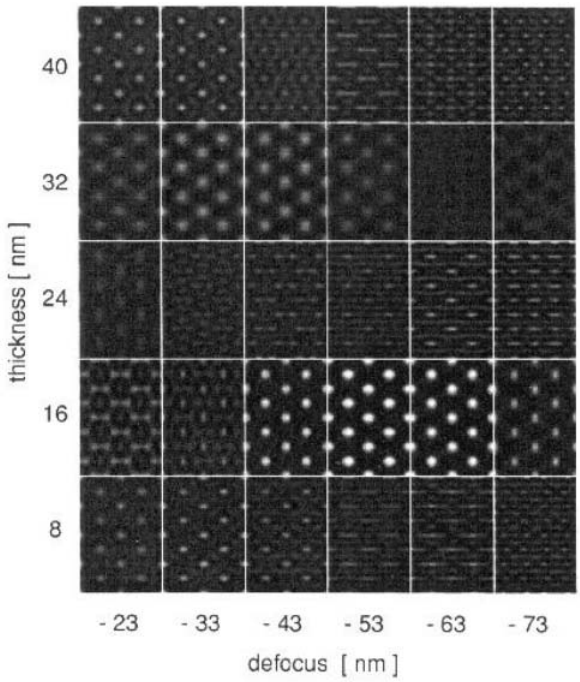

Thickness-defocus map in Fe3Al intermetallics
M. Karlik Materials structure, 8 (2001),3

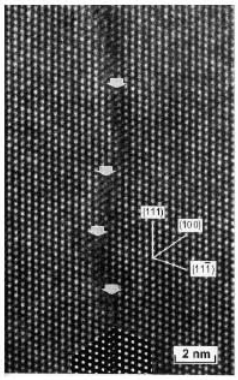

Experiment

What do you notice ?

Can you figure out the underlying explanation?

"delocalisation"

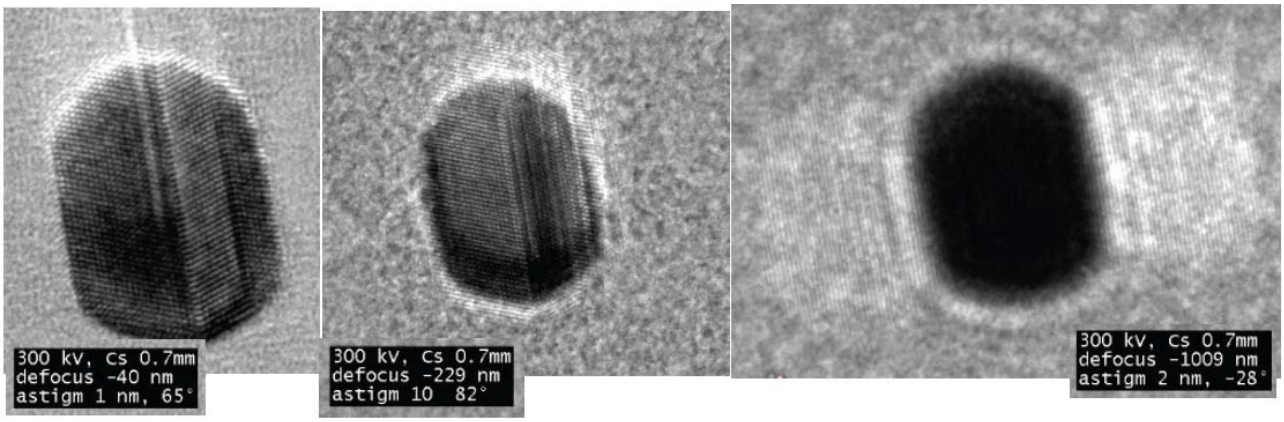

Au nanoparticle on amorphous carbon.Various defocalisation

Example: What is the secret of a relaxor…?

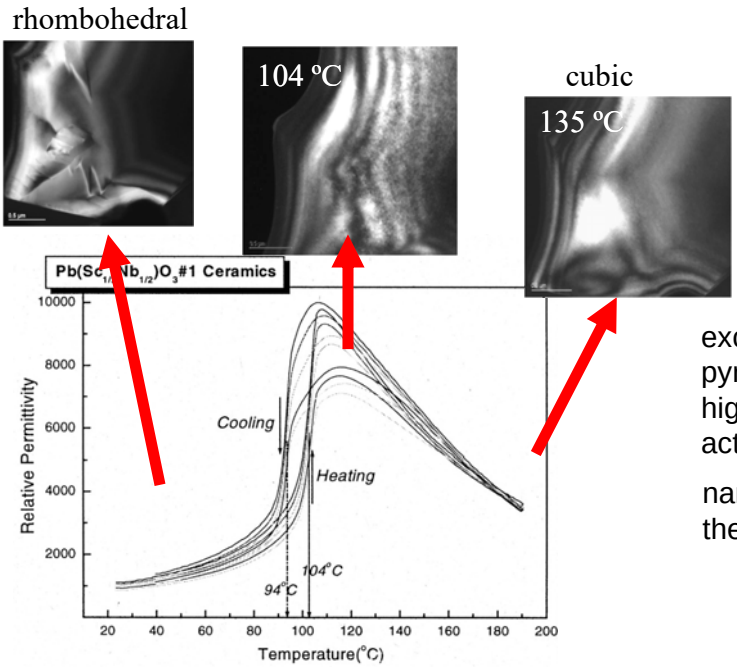

excellent dielectric, electrostrictive, and pyroelectric properties for high performance sensors and actuators

nanoscale chemical inhomogeneity in the *B*-site sublattice

direct observation of the B-site cationic order in the ferroelectric relaxor $Pb(Mg_{1/3}Ta_{2/3})O_3$ by high-resolution Transmission Electron Microscopy

The cation ordering on the B-site of $Pb(Mg_{1/3},Ta_{2/3})O_3$

perovskite

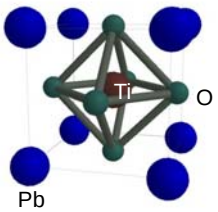

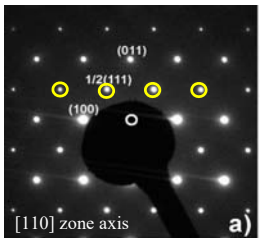

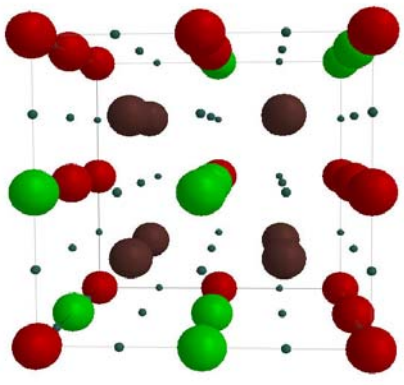

Mg and Ta randomly distributed on the different B-sites „disordered“

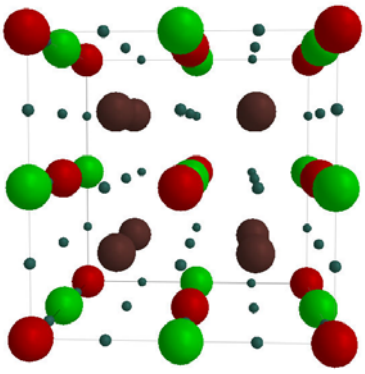

Mg and Ta occupy alternatively the different B-sites „ordered“

1:1-type superstructure

Chemical ordered regions in Pb(Mg1/3,Ta2/3)O3, two different models

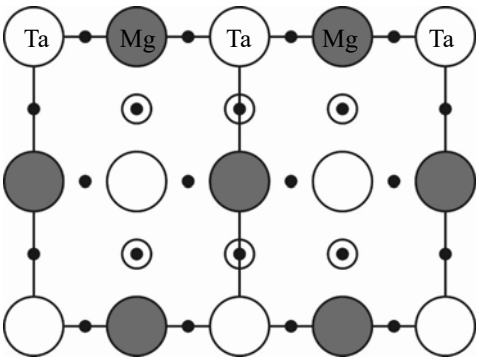

[110] direction

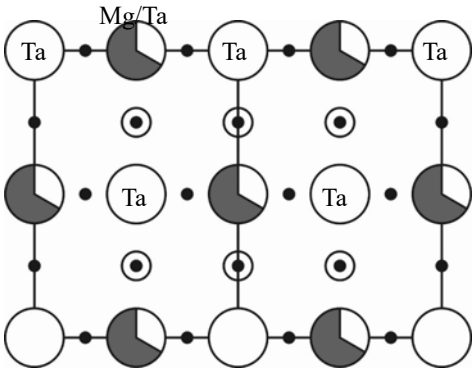

Space-charge model:
perfect 1:1 ratio in ordered regions
Mg : Ta = 1:1

Mg : Ta = 1:2

Random-site model
(also called random layer)
Perfect overall stochiometry

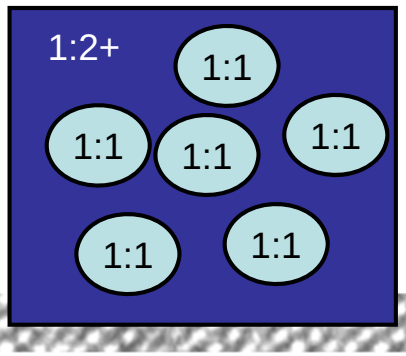

B. P. Burton and E. Cockayne, Ferroelectrics **270**, 1359 (2002).

B. P. Burton
J. Phys. Chem. Solids **61**, 327 (2000).

first-principles total energy calculations:
random-layer model is an energetically stable ground state structure

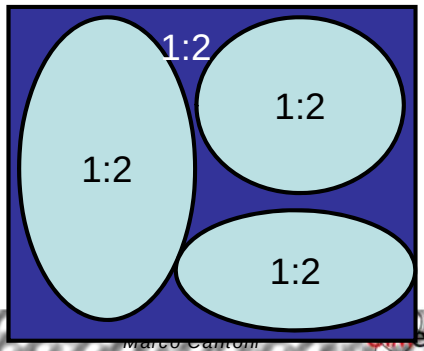

Different zone axes

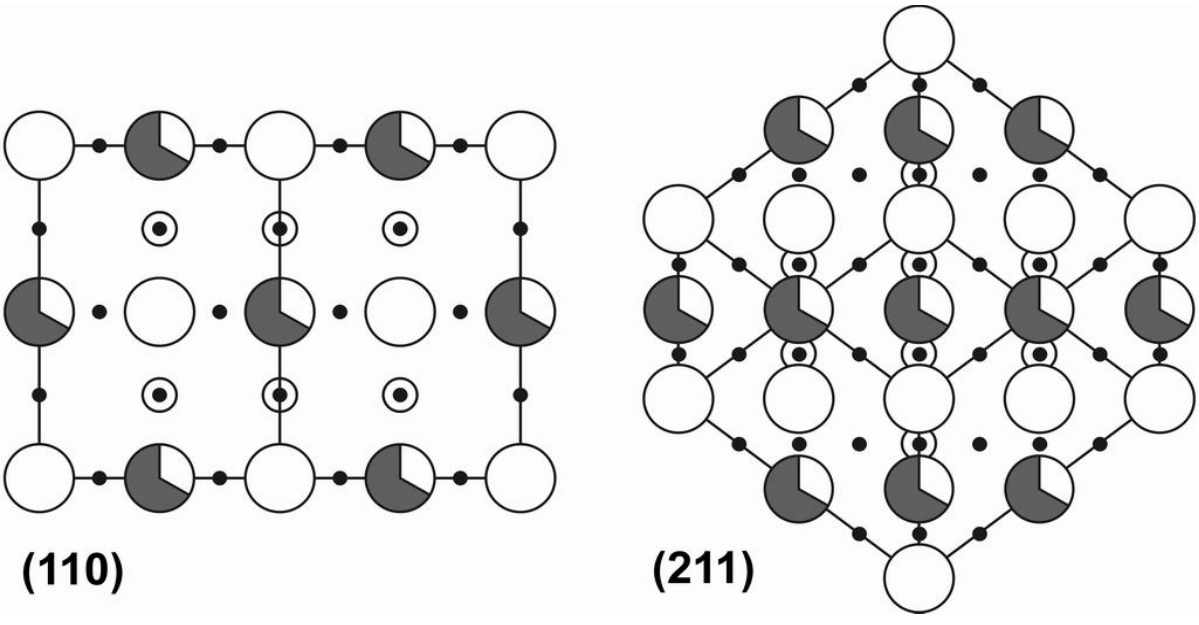

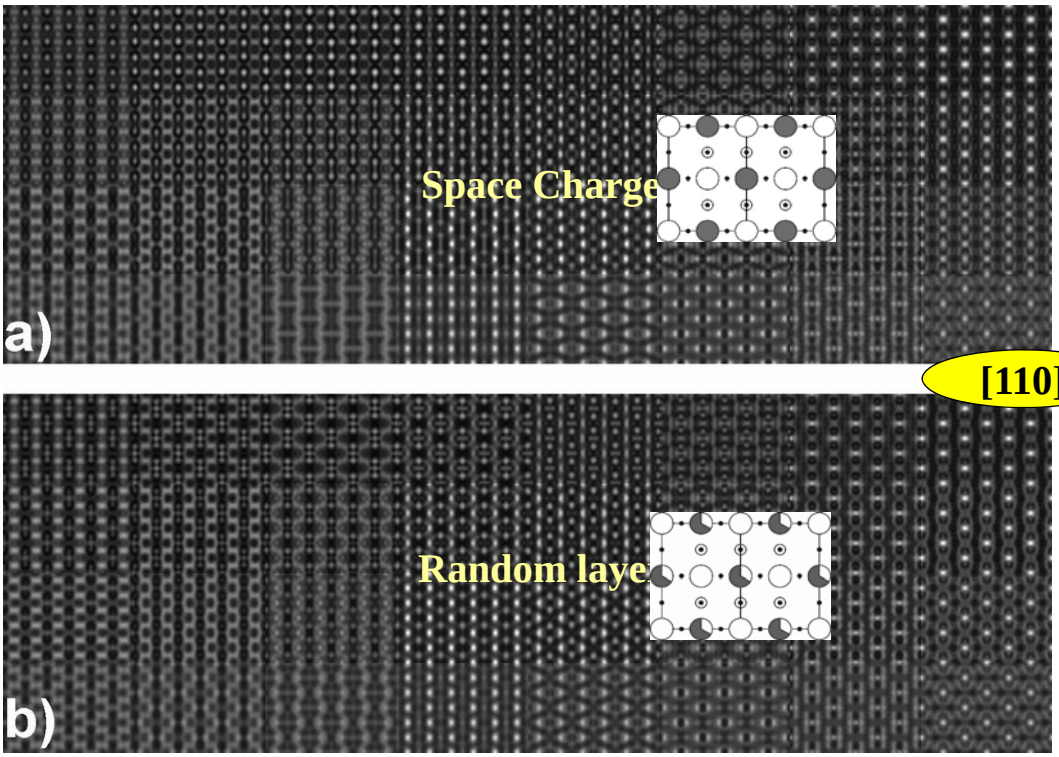

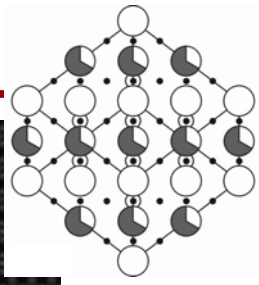

Space charge model

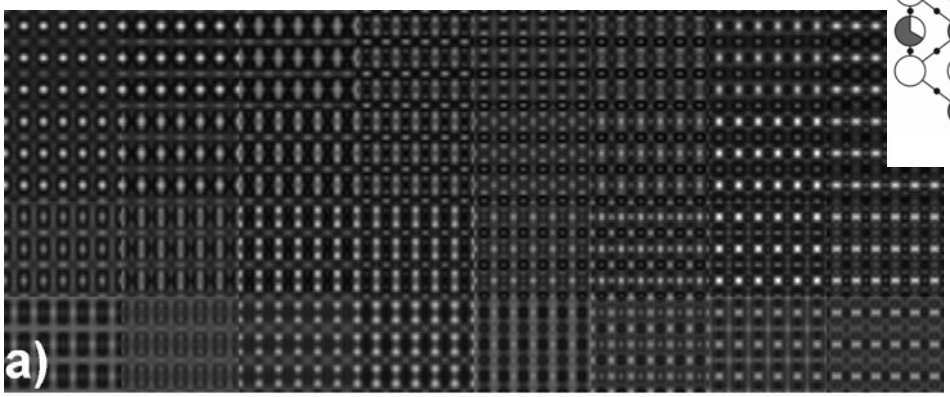

Random layer model

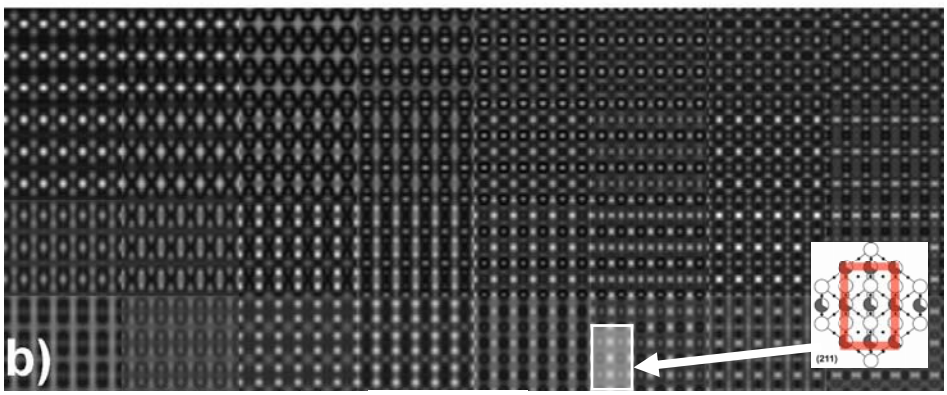

thickness

defocus

experimental image compared to simulations

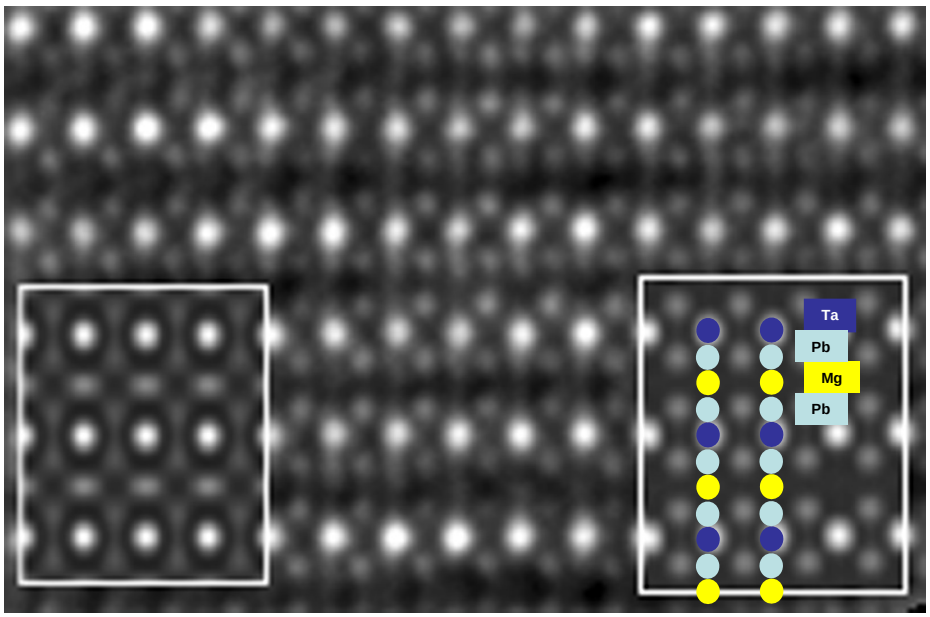

Space-charge **Random-site**

***Cantoni**, M; Bharadwaja, S; Gentil, S; Setter, N. 2004.*
Direct observation of the B-site cationic order in the ferroelectric relaxor Pb(Mg1/3Ta2/3)O-3.
JOURNAL OF APPLIED PHYSICS 96 (7): 3870-3875.

HRTEM image formation

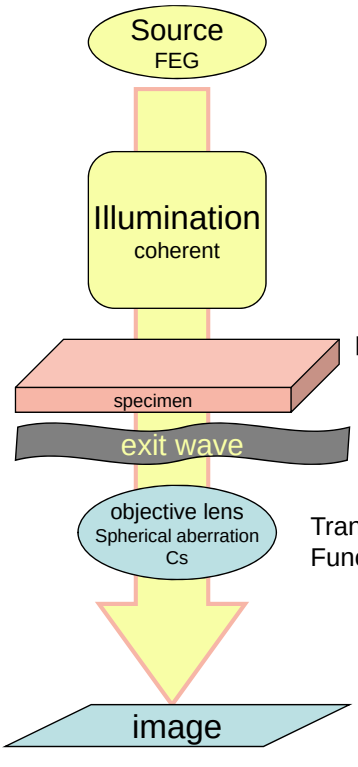

projected potential

Transfer Function

image of "projected potential"

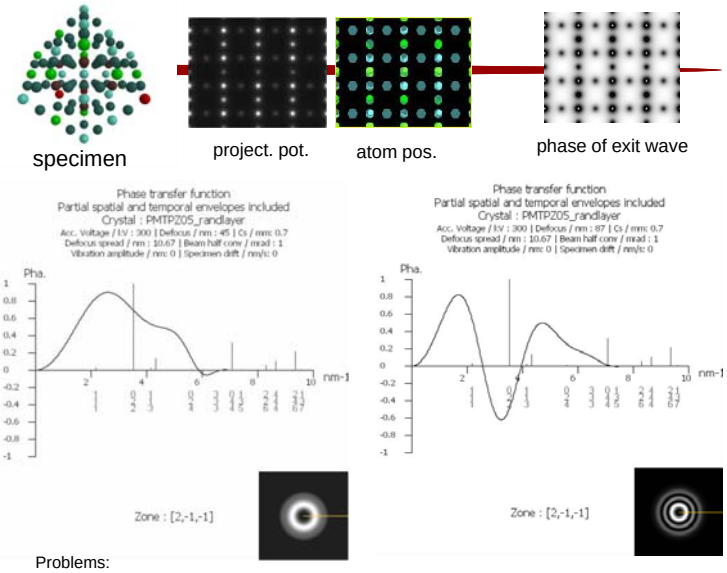

Problems:
defocusing for contrast: delocalization of information, information limit not used

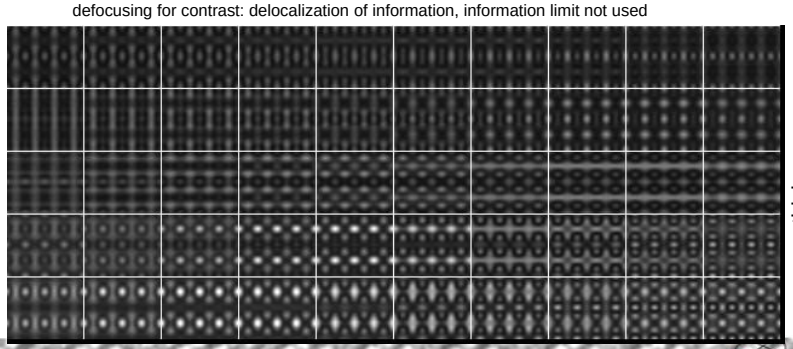

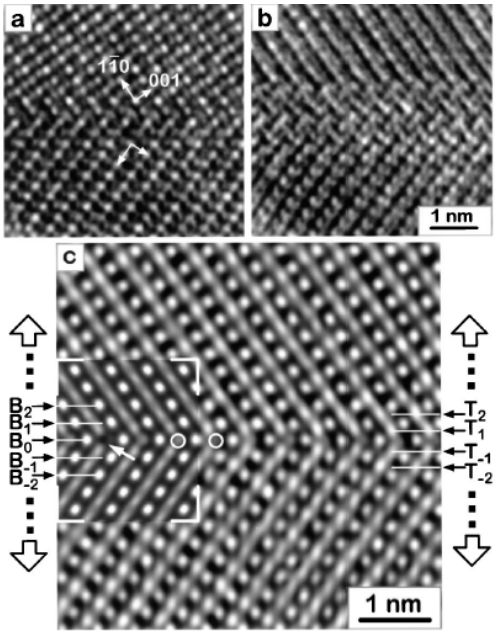

reconstructed phase of {111} twin boundary in perovskite BaTiO3

<110> zone axis. Phase of EPW reconstructed from series of 20 images with different defocus values.
The inset is a simulation for a specimen thickness of 2.8 nm. Circles denote oxygen columns located in the boundary plane. {111} Ti planes are labeled with "*T*" and {111} Ba-O planes with "*B*".

C. L. Jia and A. Thust
PHYSICAL REVIEW LETTERS 82, 25

Iterative Wave Form Reconstruction: IWFR
FEI: TrueImage

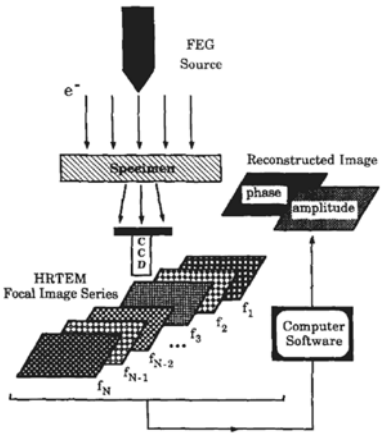

A. Thust, M.H.F. Overwijk, W.M.J. Coene, M. Lentzen
Ultramicroscopy 64 (1996) 249-264

L.J. Allen, W. McBride, N.L. O'Leary, M.P. Oxley
Ultramicroscopy 100 (2004) 91–104

Aberration Correction

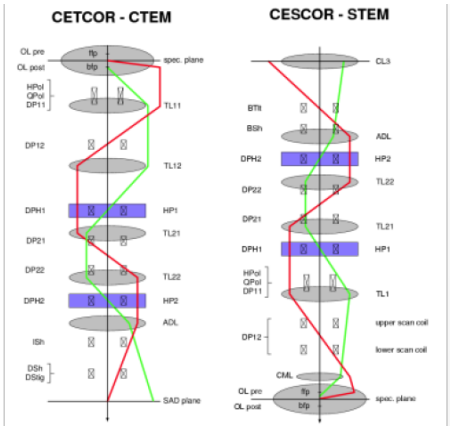

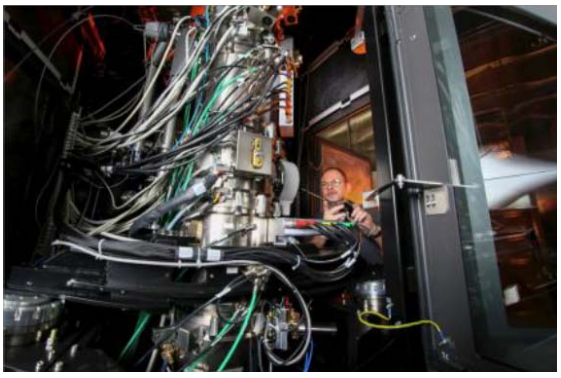

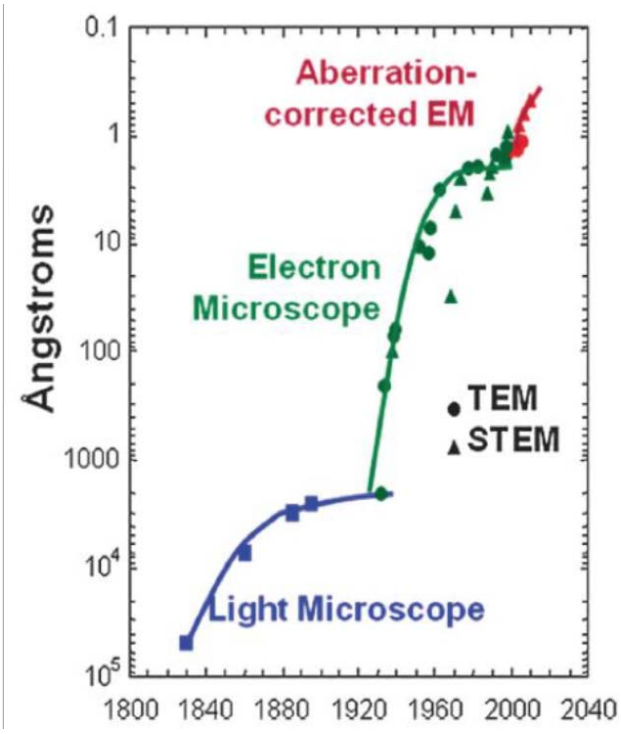

correctors

- Astigmatisme
  - Optique: correction avec une lentille cylindrique
  - EM: correction avec un stigmateur: quadrupôle
    - Image d'un point = ligne
    - Deux quadrupôles montés à 45° permettent d'ajuster la force et la direction de la correction
- Abbération sphérique
  - Optique: utilisation de lentilles avec des surfaces non-sphériques
  - EM: combinaison de quadrupôles et d'octopôles

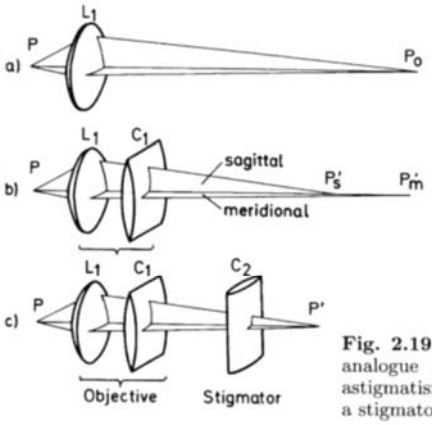

Fig. 2.19a–c. Light-optical analogue of the action of astigmatism (L1 + C1) and a stigmator C2 [2.30]

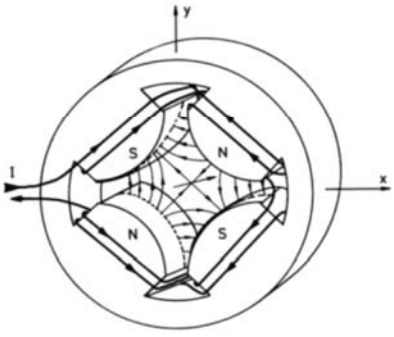

Fig. 2.12. Construction of a quadrupole lens

the aberration-corrected transmission electron microscope

(Rose, 1990; Haider et al., 1998)

Maximilian Haider, Stephan Uhlemann,
Eugen Schwan, Harald Rose, Bernd Kabius, Knut Urban
NATURE, VOL 392, 1998

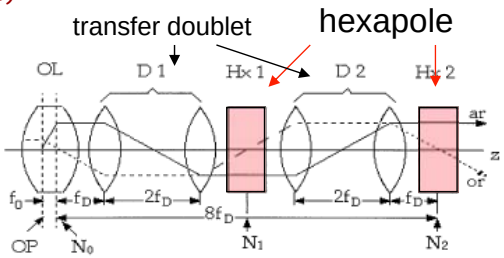

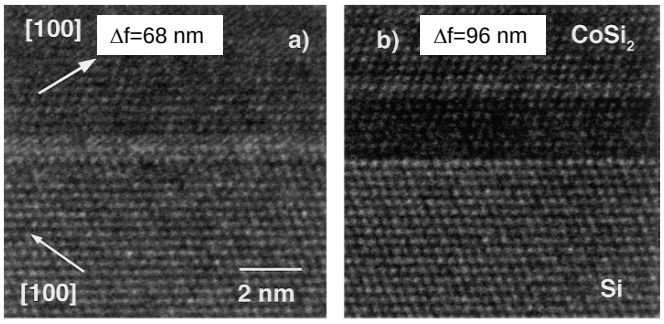

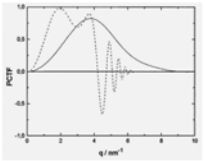

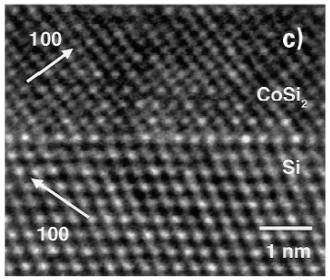

Cs-corrector

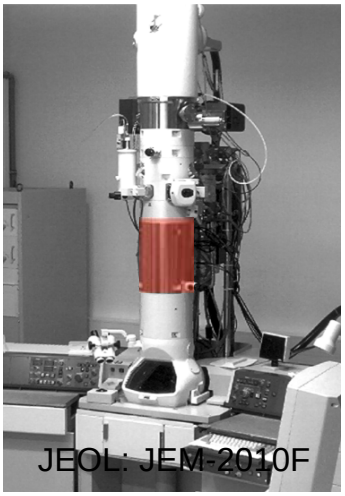

Super microscopes.....

Uncorrected with Cs=1mm

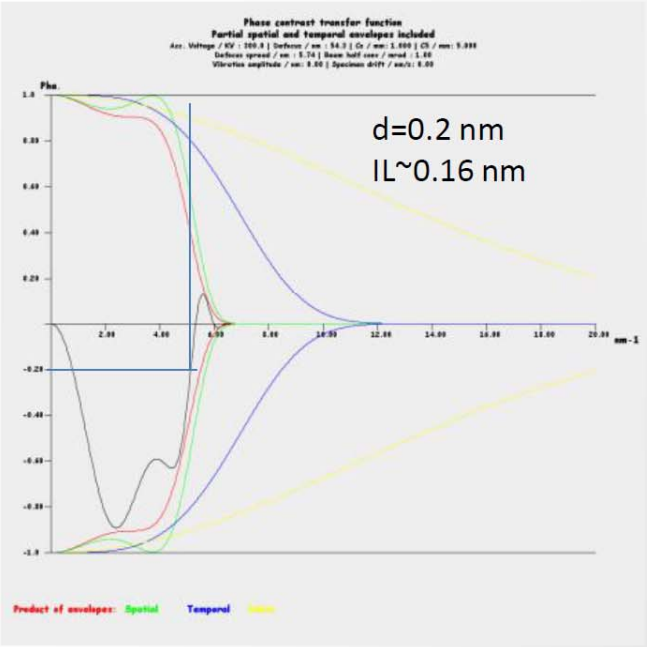

Corrected with Cs=0.01mm

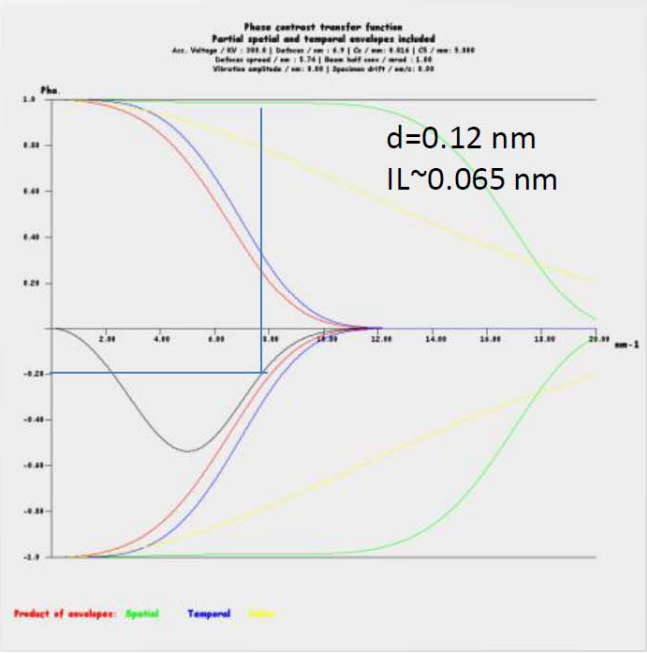

Cs correctors 2008: FEI Titan

Breaking the spherical and chromatic aberration barrier in transmission electron microscopy

B. Freitag, S. Kujawa, P.M. Mul, J. Ringnalda*, P.C. Tiemeijer

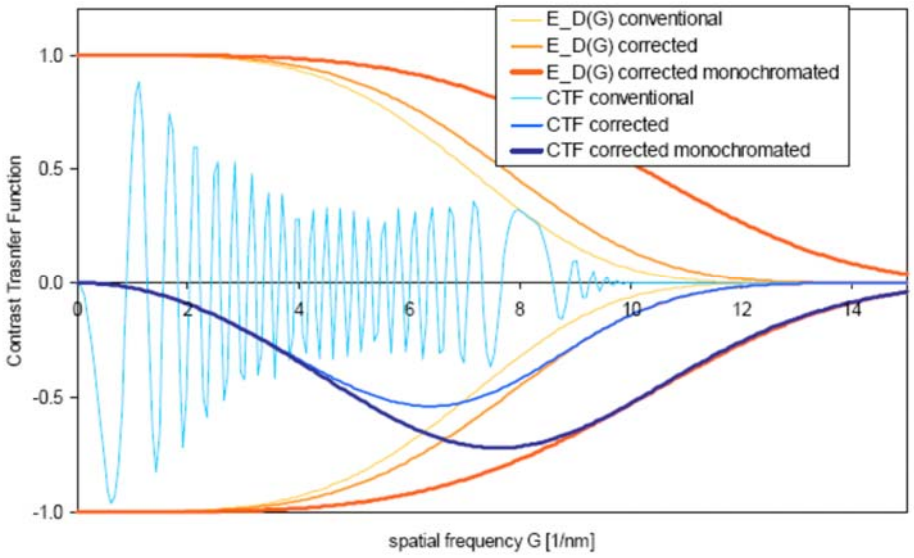

Sharp interfaces

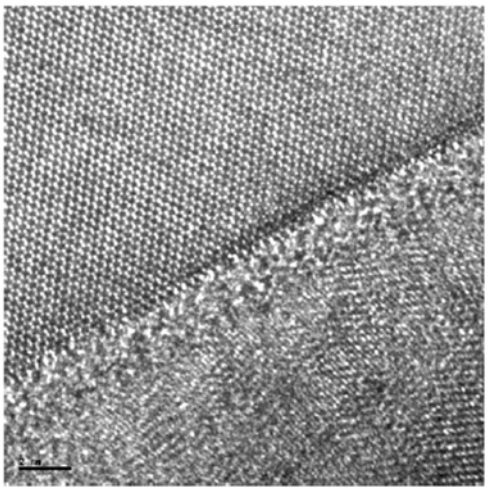

Fig. 3. TEM image of a cross section of a MOSFET transistor showing the amorphous gate oxide layer between crystalline silicon and polycrystalline silicon, recorded with monochromator on and Cs corrector on. The image was taken with 0.1 nA beam current on the CCD, 1 s exposure time, and 2 mrad half convergence angle.

No delocalisation at interfaces anymore

Cs corrector off

Cs corrector on

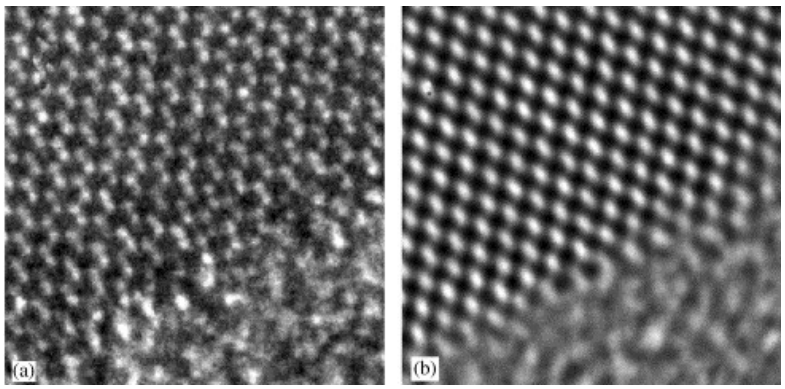

Gold crystal

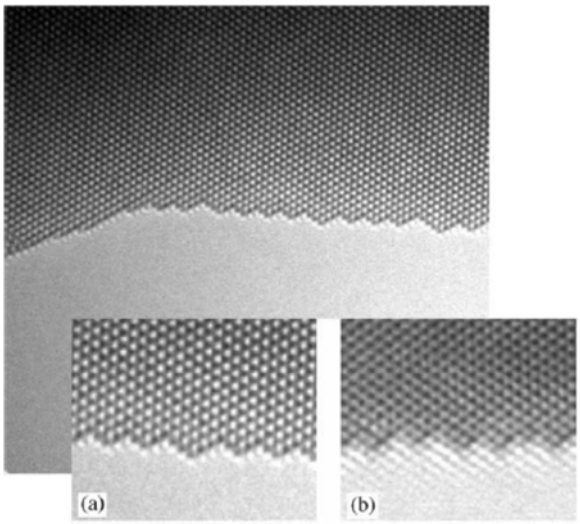

Fig. 5. Images of gold crystal recorded with monochromator on and Cs corrector on, with insets illustrating the difference between Cs corrector on and Cs corrector off: (a) The edge is clearly imaged, without fresnel fringes or delocalization effects. (b) The image without Cs correction, illustrating the difficulty of directly interpreting an image from a conventional field emission gun system.

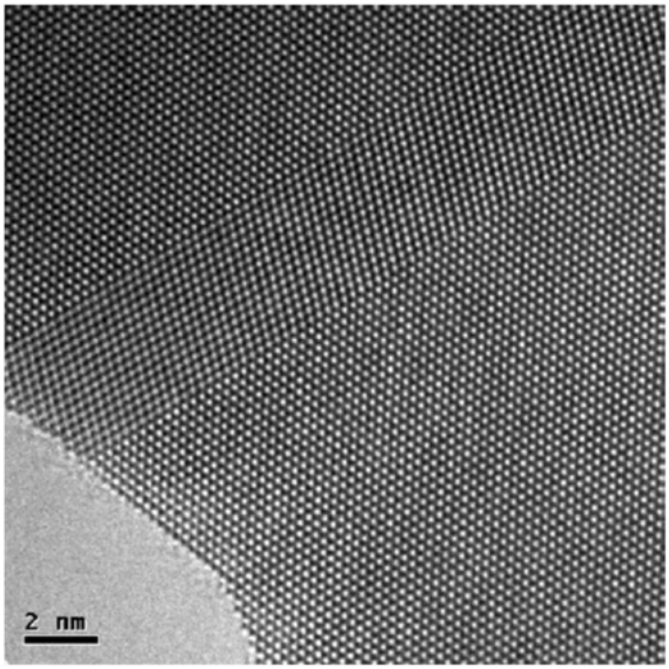

Handbook of Nanoscopy, Volume 1&2

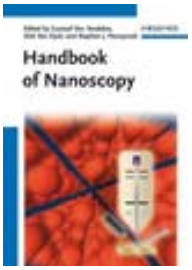

Editor(s): Gustaaf Van Tendeloo, Dirk Van Dyck, Stephen J. Pennycook
Published Online: 23 MAY 2012 05:12AM EST
Print ISBN: 9783527317066
Online ISBN: 9783527641864
DOI: 10.1002/9783527641864

3 Ultrahigh-Resolution Transmission Electron Microscopy at Negative Spherical Aberration

Knut W. Urban, Juri Barthel, Lothar Houben, Chun-Lin Jia, Markus Lentzen, Andreas Thust, and Karsten Tillmann

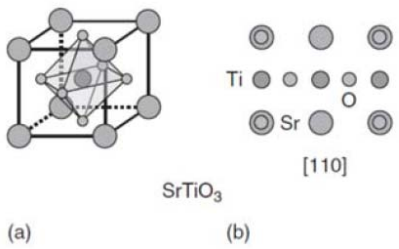

Figure 3.2 $SrTiO_3$. (a) Perspective view of the unit cell. (b) Projection along the [110] crystal direction. In this viewing direction, three types of atomic columns are distinct, which are occupied alternatively with strontium and oxygen, with titanium, and with oxygen atoms.

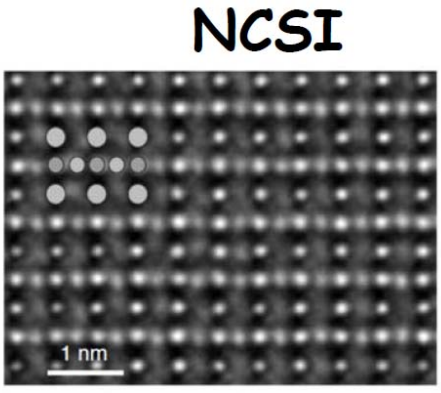

Figure 3.3 Experimental image of $SrTiO_3$ taken along the [110] zone axis employing the NCSI technique (FEI Titan 80–300 with imaging corrector, operated at 300 keV). All three atomic species are visible (compare inset) at bright contrast on a dark background.

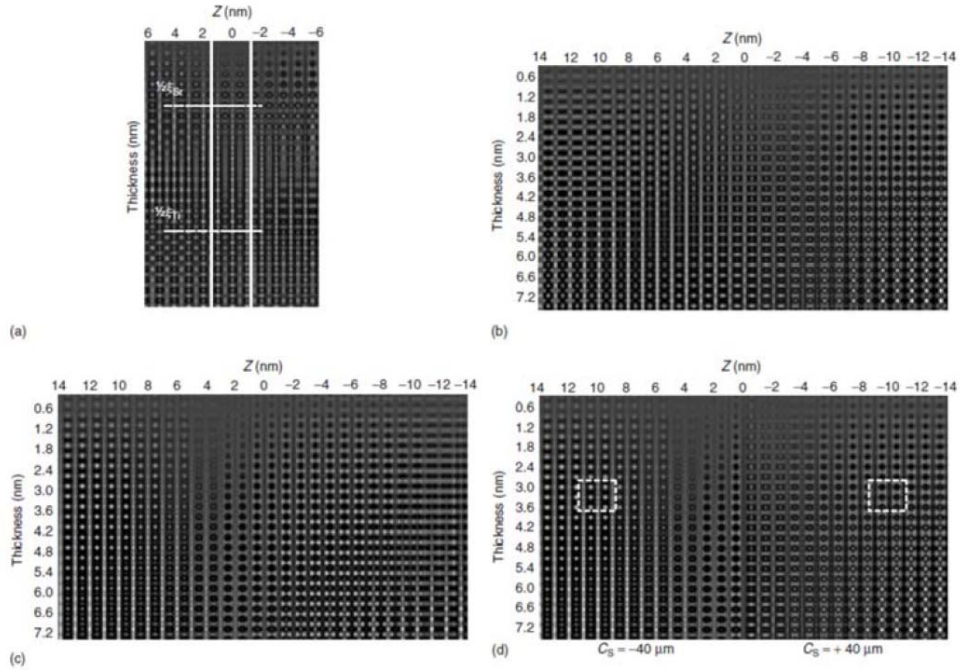

Figure 3.4 Simulated images for $SrTiO_3$ [110] at 200 keV. The composite shows a single unit cell in [110] projection for different defocus values Z and sample thicknesses at an electron energy of 200 keV for the spherical aberration parameter C_S = 0 nm, +40 µm, and −40 µm (a–c). (d) Direct comparison of the positive and negative C_S situation, where in the $-C_S$ case overfocus (positive values of Z) and in the positive C_S case the usual underfocus (negative values of Z) is applied. The frame is used as a guide for the eye for same sample thickness.

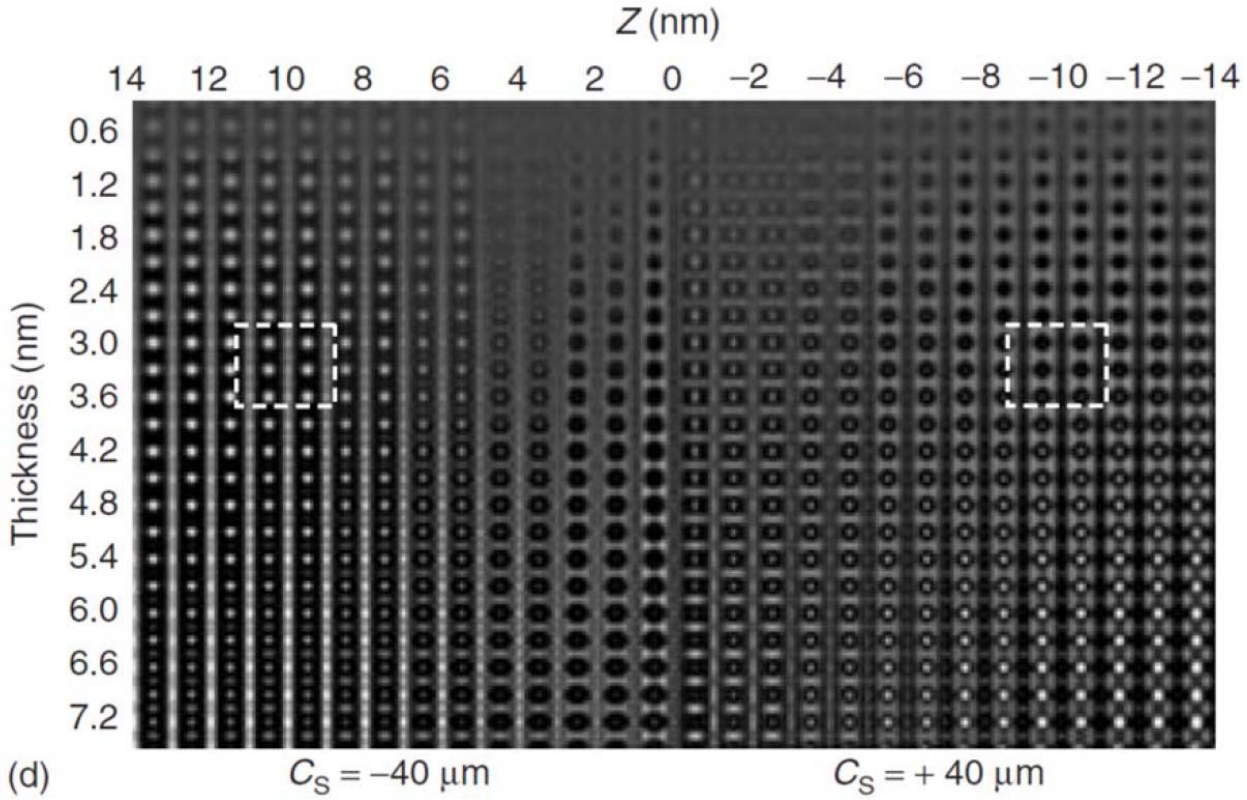

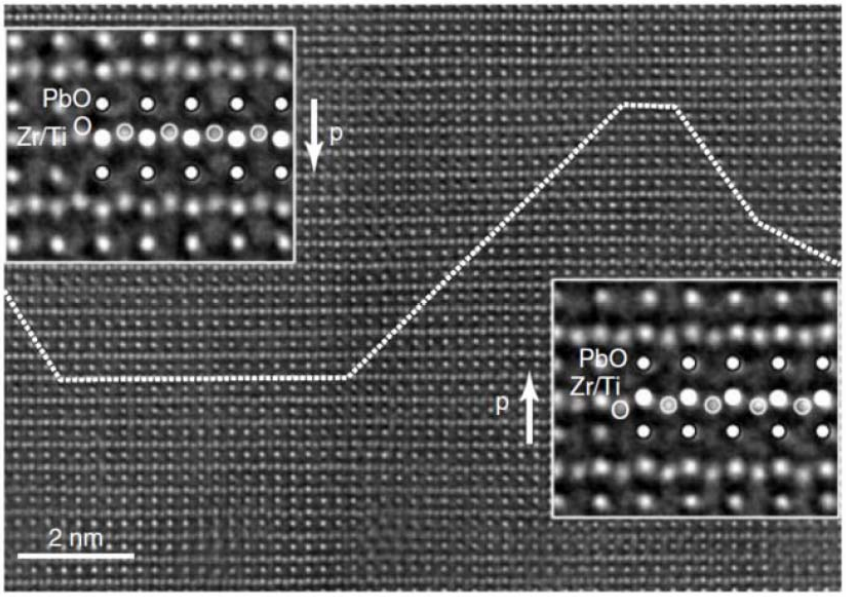

Figure 3.13 $Pb(Zr_{0.2}Ti_{0.8})O_3$ imaged along the [110] direction. The inset on the left shows that the horizontal Zr/Ti atom rows are shifted toward the respective Pb atom row above the Zr/Ti row. Oxygen is shifted even more, thus becoming no longer colinear with the Zr/Ti rows. This indicates that the material is ferroelectrically polarized. The polarization vector **p** points downward. The inset on the right shows opposite atomic shifts. The direction of the polarization vector there is upward. The dotted line shows the appertaining ferroelectric inversion domain wall. With respect to the atomic structure, the inclined domain-wall sections consist of vertical transversal and horizontal longitudinal domain-wall segments. As a result they are uncharged. The horizontal sections are longitudinal domain walls, which are charged [56].

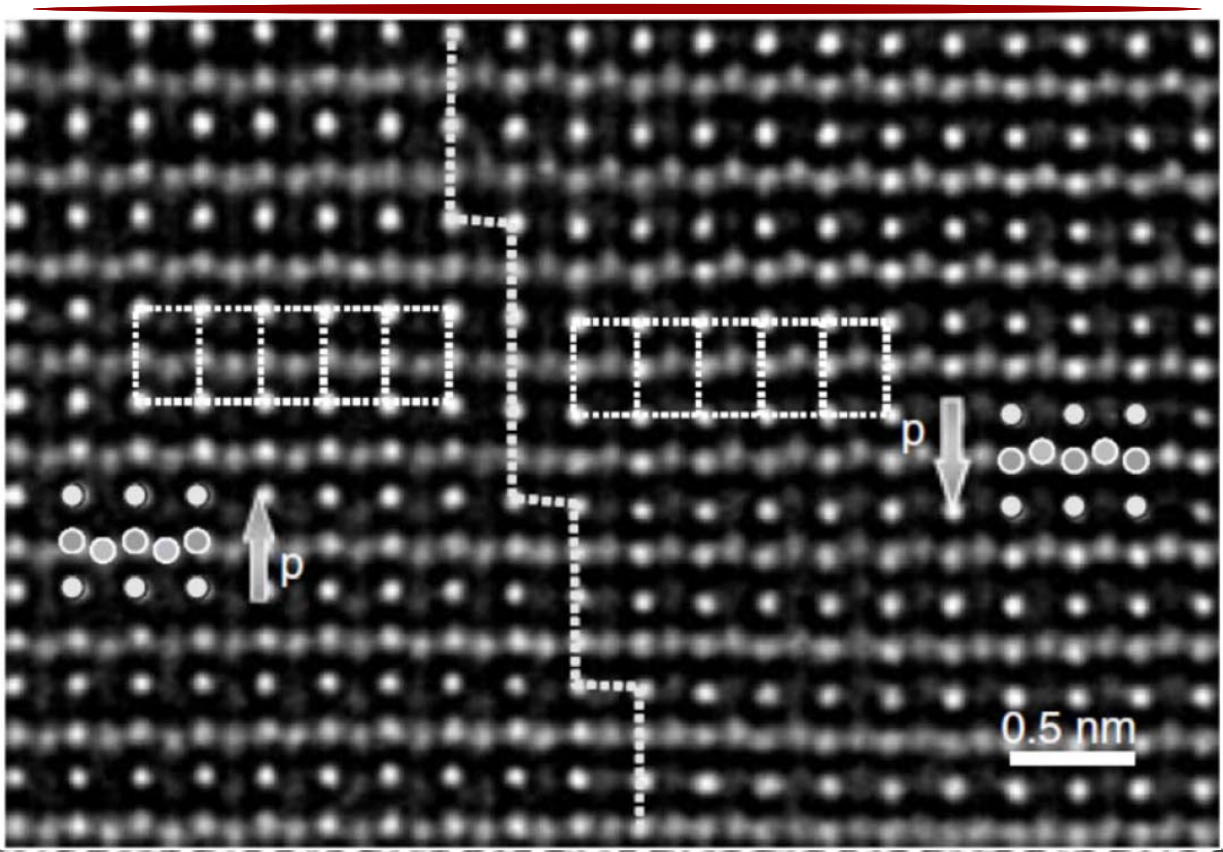

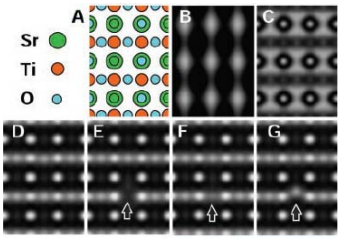

simulation

200kV, cs corrected TEM

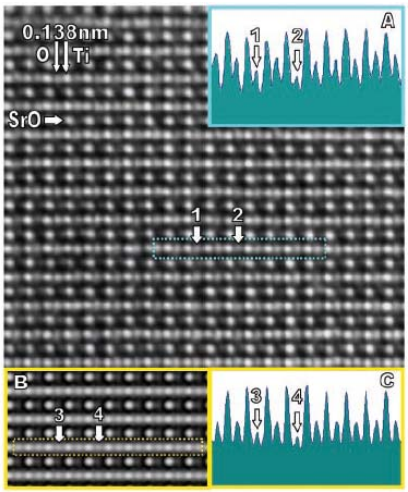

Experimental image

Atomic-Resolution Imaging of Oxygen in $SrTiO_3$
C.-L. Jia, M. Lentzen, K. Urban
SCIENCE VOL 299 (2003)

- direct imaging of heavy and light atoms in a sinlge image
- No delocalisation: atoms are seen at their real position

Oxygen vacancies in $YBa_2Cu_3O_x$

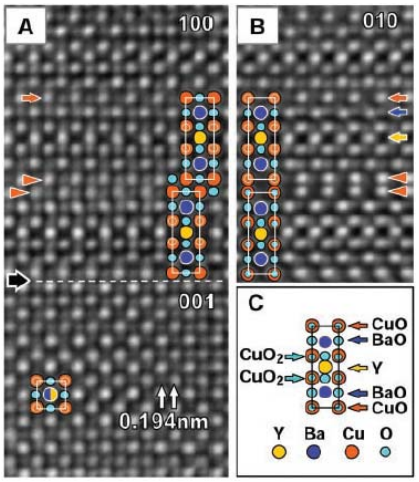

Chun-Lin Jia, Markus Lentzen, and Knut Urban
Microsc. Microanal. 10, 174–184, 2004